



## AN INVESTIGATION OF AUTOFRETTAGING LOOSE LINERS INTO THICK SHELLS – THEORY AND EXPERIMENT

VON KÁRMÁN GAS DYNAMICS FACILITY  
ARNOLD ENGINEERING DEVELOPMENT CENTER  
AIR FORCE SYSTEMS COMMAND  
ARNOLD AIR FORCE STATION, TENNESSEE 37389

March 1976

Final Report for Period December 1972 – October 1974

Approved for public release; distribution unlimited.

Prepared for

DIRECTORATE OF TEST (XO)  
ARNOLD ENGINEERING DEVELOPMENT CENTER  
ARNOLD AIR FORCE STATION, TENNESSEE 37389

## NOTICES

When U. S. Government drawings specifications, or other data are used for any purpose other than a definitely related Government procurement operation, the Government thereby incurs no responsibility nor any obligation whatsoever, and the fact that the Government may have formulated, furnished, or in any way supplied the said drawings, specifications, or other data, is not to be regarded by implication or otherwise, or in any manner licensing the holder or any other person or corporation, or conveying any rights or permission to manufacture, use, or sell any patented invention that may in any way be related thereto.

Qualified users may obtain copies of this report from the Defense Documentation Center.

References to named commercial products in this report are not to be considered in any sense as an endorsement of the product by the United States Air Force or the Government.

This report has been reviewed by the Information Office (OI) and is releasable to the National Technical Information Service (NTIS). At NTIS, it will be available to the general public, including foreign nations.

## APPROVAL STATEMENT

This technical report has been reviewed and is approved for publication.

FOR THE COMMANDER



CARL J. SCHULZE  
Major, USAF  
Chief Air Force Test Director, VKF  
Directorate of Test



CRAIG E. MAHAFFY  
Colonel, USAF  
Director of Test

**UNCLASSIFIED**

# **UNCLASSIFIED**

## **20. ABSTRACT (Continued)**

large enough to reline with a low cost, low carbon, steel tube. The liner is autofrettaged into place; however, some difficulty has been experienced in predicting the pressure required to firmly seat the liners. The purpose of the study reported herein was to determine a more accurate way to predict adequate autofrettage pressures. In the work reported, a 10-in.-long section of a high-pressure launch tube was used to simulate the actual procedure. Contact pressure between the shell and the liner was monitored by means of strain gages cemented to the outside of the outer shell. Variables such as liner-shell clearance, pressure level, pressure-holding time, outside diameter of the outer shell, and pressure cycling were considered. Of these variables only the pressure level and the outside diameter of the outer shell had any marked effect on liner seating.

## PREFACE

The work reported herein was conducted by the Arnold Engineering Development Center (AEDC), Air Force Systems Command (AFSC), under Program Element 65807F. The results of the research were obtained by ARO, Inc. (a subsidiary of Sverdrup & Parcel and Associates, Inc.), contract operator of AEDC, AFSC, Arnold Air Force Station, Tennessee. The work was done under ARO Project Number V45G. The authors of this report were Dennis T. Akers and Gerald F. Gillis, ARO, Inc. The manuscript (ARO Control No. ARO-VKF-TR-75-79) was submitted for publication on June 16, 1975.

## CONTENTS

	<u>Page</u>
1.0 INTRODUCTION . . . . .	7
2.0 OVERSTRAINING PROCEDURES AND SETUP FOR RELINING ACTUAL LAUNCH TUBES . . . . .	10
3.0 AUTOFRETTAGE TEST ARTICLE DESCRIPTION . . . . .	16
4.0 DESCRIPTION OF TEST PROCEDURE AND EQUIPMENT	
4.1 Equipment . . . . .	17
4.2 Procedure . . . . .	19
4.3 Selection of Maximum Autofrettage Pressure . . . . .	20
4.4 Original Dimensions of the Test Pieces . . .	20
4.5 Interpretation of Strain-Gage Readings . . .	21
5.0 DISCUSSION OF TEST RESULTS	
5.1 Effect of Pressure-Holding Time . . . . .	21
5.2 Effect of Pressure Cycling . . . . .	22
5.3 Effect of Liner Clearance . . . . .	24
5.4 Effect of Pressure Level . . . . .	25
5.5 Effect of Launch Tube Outside Diameter . . .	27
6.0 PREDICTION OF THE HOLDING FORCE PRODUCED BY AUTOFRETTAGING . . . . .	28
7.0 COMPARISON OF EXPERIMENTAL RESULTS WITH THEORY . . . . .	30
8.0 MISCELLANEOUS OBSERVATIONS	
8.1 Discrepancies in Contact Pressure . . . . .	34
8.2 Liner Length Changes . . . . .	34
8.3 Application of Results to Other Liners . . .	35
9.0 CONCLUSIONS . . . . .	35
REFERENCES . . . . .	36

## ILLUSTRATIONS

### Figure

1. Upstream End Closure for Overstraining a Relined 7-in.-OD Launch Tube . . . . .	12
2. Muzzle End Closure for Overstraining a Relined 7-in.-OD Launch Tube . . . . .	12
3. Upstream End Closure for Overstraining the Modified Version of the 7-in.-OD Relined Launch Tube . . . . .	14
4. High-Pressure Section to Launch Tube Joint . .	14
5. Pressure Time Trace for Relined Launch Tube (Serial No. 018) . . . . .	15

<u>Figure</u>	<u>Page</u>
6. Assembly of Test Article . . . . .	16
7. Schematic of Test Setup . . . . .	18
8. Photographs of Test Setup . . . . .	18
9. Circumferential Strain at the OD of a 7-in. Shell as a Function of Time Using a Medium- Fit (0.020-in. Clearance) Liner . . . . .	22
10. Circumferential Strain at the OD of a 7-in.-OD Shell as a Function of Internal Pressure Using a Medium-Fit (0.020-in. Clearance) Liner. . . . .	23
11. Residual Strain as a Function of Internal Pressure . . . . .	26
12. Required Autofrettage Pressure for Any Size Shell with a 3-in. ID . . . . .	28
13. Comparison of Theoretical to Experimental Axial Force . . . . .	29
14. Comparison of Theoretical to Experimental Liner-Shell Contact Pressure for 5.5-in.-OD Shell with Medium-Fit (0.0181-in. Clearance) Liner. . . . .	32
15. Comparison of Theoretical to Experimental Liner-Shell Contact Pressure for a 7-in.-OD Shell with Various Liners . . . . .	32
16. Comparison of Theoretical to Experimental Liner-Shell Contact Pressure for a 9-in.-OD Shell with Medium-Fit (0.0173-in. Clearance) Liner . . . . .	33
17. Comparison of Theoretical to Experimental Liner-Shell Contact Pressure for an 11-in.-OD Shell with Medium-Fit (0.0181-in. Clearance) Liner . . . . .	33

#### TABLES

1. Measurements of Liner Movement for 013 Launch Tube . . . . .	39
2. Measurements of Liner Movement for 011 Launch Tube . . . . .	39
3. Dimensions of Components Tested . . . . .	40

	<u>Page</u>
4. 7-in.-OD Shell with Medium-Fit Liner (0.020-in. Clearance) Tested for the Effect of Pressure Hold Time (Test No. 1) . . . . .	41
5. 7-in.-OD Shell with Medium-Fit Liner (0.020-in. Clearance) Tested for the Effect of Hold Time and Pressure Cycles (Test No. 2) . .	42
6. 7-in.-OD Shell with Medium-Fit Liner (0.0185-in. Clearance) Tested for the Effect of Liner Clearance (Test No. 3) . . . . .	50
7. 7-in.-OD Shell with Tight-Fit Liner (0.0105-in. Clearance) Tested for the Effect of Liner Clearance (Test No. 7) . . . . .	52
8. 7-in.-OD Shell with Tight-Fit Liner (0.0105-in. Clearance) Tested for the Effect of Liner Clearance (Test No. 9) . . . . .	53
9. 7-in.-OD Shell with Loose-Fit Liner (0.024-in. Clearance) Tested for the Effect of Liner Clearance (Test No. 8) . . . . .	54
10. 7-in.-OD Shell with Loose-Fit Liner (0.0245-in. Clearance) Tested for the Effect of Liner Clearance (Test No. 10) . . . . .	55
11. 5.5-in.-OD Shell with Medium-Fit Liner (0.0181-in. Clearance) Tested for the Effect of Launch Tube OD (Test No. 5) . . . . .	56
12. 9-in.-OD Shell with Medium-Fit Liner (0.0173-in. Clearance) Tested for the Effect of Launch Tube OD (Test No. 6) . . . . .	57
13. 11-in.-OD Shell with Medium-Fit Liner (0.0181-in. Clearance) Tested for the Effect of Launch Tube OD (Test No. 4) . . . . .	58
14. Liner and Shell Dimensions after Completion of Axial-Force Test . . . . .	61
15. Typical Liner Dimension Changes during Testing . . . . .	61

#### APPENDIXES

A. BASIC STRESS EQUATIONS . . . . .	63
B. CALCULATION OF CONTACT PRESSURE FROM MEASURED STRAIN-GAGE DATA . . . . .	76
NOMENCLATURE . . . . .	77

## 1.0 INTRODUCTION

Free-flight test work at AEDC has primarily been done in the Hyperballistic Ranges (G) and (K) of the von Kármán Gas Dynamics Facility (VGF). The test usually involves a model and a sabot launched at very high velocities. The model launcher typically involves a 35-ft-long, 2.5-in.-inside diameter (ID), smooth bore, launch tube. Due to high model-sabot acceleration loads, occasional failures occur causing local gouging or cratering of the launch tube bore.

Since launch tubes are very expensive (20 to 30 thousand dollars), several methods of repairing them have been considered. Local welding was investigated but the high-carbon content of the material (0.28 to 0.38, National Forge alloy NA-14) caused cracking around the welds. Another method of using molten powdered filler material was discarded because of poor adherence to the parent metal. Still another method considered involved boring out the launch tube to a new ID and relining with a high-strength liner. The idea was to use a shrink-fit or tight-fit construction and a liner of sufficient strength to withstand the pressure. Upon further consideration, it became apparent that the liner would be expensive, require close tolerance machining on both the outside diameter (OD) and ID, require difficult assembly operations, and the liner would also have a high-carbon content which would rule out weld repair if it became damaged. Thus, the method finally used was to bore out the launch tube and autofrettage a low-carbon, low-strength, expendable liner into the launch tube. The material selected was 1026 steel which is readily weldable and thus could be repaired by the "Firecracker" welding technique (Ref. 1).

The procedure adopted was to assemble the two shells as a loose fit and plastically swell the inner one into the outer shell with an internal pressure. To be acceptable, a tight interference had to be achieved so that no sliding between the two shells would occur under the high axial acceleration loads sustained during firing. If sliding occurred, a gap would open up between the launch tube and high-pressure section, damage the sabot, and possibly cause a launch failure and tube damage.

Another requirement was to keep the liner thin to minimize material removal from the outer shell. In the event of a liner failure, the outer shell would have to safely contain the pressure. In contrast, a reasonable liner thickness was required to permit machining in 35-ft lengths. A nominal 0.25-in. wall was selected as a reasonable liner.

Preliminary discussions with the supplier of the liner material revealed that they could supply rolled, resistance welded, cold worked, 1026 carbon steel liners with nominal inside and outside diameters of 2.5 and 3.0 in. The material has a specified yield strength of 75,000 psi and an ultimate of 85,000 psi. These liners were secured to one-half commercial straightness (0.015 in any three feet as measured on a surface plate with a feeler gage) at a cost of \$2.25 per foot. The tube OD was then centerless ground to close tolerance at a cost of \$1.40 per foot. The centerless grinding duplicated the out-of-straightness (waviness) of the tube as fabricated and resulted in a constant wall thickness liner.

Obviously, the lack of straightness could produce some interference on insertion of the liner into the tube. For example, if the liner had the maximum bow of 0.005 in./ft from one end to the other, the maximum deviation at the center would be 0.0875 in. Based on a centrally loaded, simply supported beam analogy, the lateral force required at the center to bend the liner enough to correct this straightness deviation would be

$$N = \frac{48EI}{\ell^3} y \quad (1)$$

where

$$\begin{aligned} E &= \text{modulus of elasticity} = 1b/in.^2, \\ I &= \text{moment of inertia} = in.^4, \\ \ell &= \text{length of the liner} = in. \end{aligned}$$

and

$$y = \text{required deflection} = in.$$

Half this value would be necessary at each end. If no clearance were provided,

$$N = \frac{48(30 \times 10^6) \pi/64 (3^4 - 2.5^4) (0.0875)}{(35 \times 12)^3}$$

$$N = 3.5 \text{ lb.}$$

An axial force would have to be applied to overcome the friction generated by the above. This force would be

$$F = \mu N + 2 \left( \mu \frac{N}{2} \right) = 2 \mu N \quad (2)$$

where

$\mu$  = coefficient of friction.

For a coefficient of friction of 0.2,

$$F = 2 (0.2) (3.5) = 1.4 \text{ lb.} \quad (3)$$

A worse case could be created by the deadweight deflection of the tube. Again assuming a simply supported tube, this deflection would be about 4.2 in. The lateral force required at the center to correct this deviation would be

$$N = 168 \text{ lb}$$

The resulting friction force would be

$$F = 67 \text{ lb.}$$

These are, of course, trivial forces; however, there are other conditions that could be worse. Probably, the worst case would be a complete reversal of curvature every three feet with a 0.015-in. deviation every three feet. Allowance was made for this condition in the clearance between the liner and launch tube. In addition, a maximum of 0.013-in. diametrical clearance appeared reasonable for easy assembly of the liner into the launch tube. Hence, the initial calculations were based on the assumption that the liner might have to grow plastically as much as 0.028 in.

From Eq. (A-36), the pressure required to fully yield the liner was calculated to be

$$P_f = 12,990 \text{ psi.} \quad (4)$$

From Eq. (A-4), the pressure required to close the 0.028-in. diametrical gap was calculated to be

$$P_i = 72,500 \text{ psi.} \quad (5)$$

Hence, if the shell remained elastic, a pressure of 72,500 psi would be just sufficient to close the 0.028-in. diametrical gap. Since this pressure is greater than full wall yield pressure, the liner would become completely plastic before the gap could be closed and should plastically flow

into intimate contact with the outer shell provided it has sufficient ductility. This plastic flow would require an elongation on the part of the liner of

$$\text{Percent elongation} = \frac{0.028}{3.0} (100 \text{ percent}) \quad (6)$$

$$= 0.93 \text{ percent.}$$

The deflection of the liner launch tube assembly during firing would have to be superposed onto this value to obtain the total elongation requirements of the liner. Preliminary calculations revealed that an additional 0.47-percent elongation would be required in the worst case (7-in.-OD launch tube with  $P_i = 75,000 \text{ psi}$ ). Thus, the total elongation required of the liner would be 1.4 percent. The specification for the material required a minimum value of three-percent elongation to provide some margin of safety.

In relining the launch tubes, questions arose as to the pressure level required to firmly seat the liner against the outer shell, required hold time at this pressure level, advantages of multiple cycles to this pressure level, and the liner-to-shell clearance that would permit easy assembly of the parts yet not be so great as to prevent firm seating of the liner or straining of the liner beyond its capability. Arbitrary combinations of these parameters were initially chosen that involved a rather lengthy procedure. Also, some slippage of the liners relative to the outer shell occurred during usage of the first two relined launch tubes. It became apparent that a more precise and more productive technique needed to be developed.

A test program was initiated to generate the information needed. Short vessels (about ten inches long) were designed, relined, and pressurized to simulate actual launch tube relining. The results of this program are summarized in the following.

## **2.0 OVERSTRAINING PROCEDURES AND SETUP FOR RELINING ACTUAL LAUNCH TUBES**

The first launch tube relined was 7-in. OD and was fabricated from NA 14 which had a yield strength of 155,000 psi and an ultimate of 168,000 psi. Three liners were prepared with the following specified outside diameters in inches:

Liner 1 2.978/2.975,  
Liner 2 2.985/2.982, and  
Liner 3 2.993/2.990.

The specification for the honing of the launch tube required an ID of 3.000 to 2.998; however, the as-machined diameter measured from 3.000 to 3.003 in. The idea was to try various clearances to determine the minimum one that could be easily assembled. (Experience has since shown that either of the three liners may be inserted in the launch tube with no difficulty.)

A light film of oil was applied to liner No. 2 and it was assembled with a launch tube as shown in Figs. 1 and 2. A craftsman was able to slide the liner into the tube with no difficulty. Rather than try a liner with less clearance, a decision was made to proceed with the medium clearance one as a first test of the overstraining concept.

The assembly was pressurized to 50,000 psi, held at pressure for about 15 minutes, and cycled three times. The 50,000 psi was arbitrarily chosen as a value below bore yield of the outer shell and sufficiently higher than the full-wall yield of the liner (12,990 psi).

On disassembly after pressurization, it was evident that plastic flow had taken place because the liner was swaged into the cap shown in Fig. 1. Efforts to drive the nut off caused the liner to slip relative to the launch tube. The apparatus was reassembled and pressurized to 71,500 psi by continuously pumping for four hours. The 71,500-psi pressure was selected as the maximum that could be applied without some yielding of the outer shell. The thought was that if yielding of the outer shell occurred it would not return to its original dimensions and the maximum interference pressure would not be developed between the two.

After this second pressurization, the liner appeared to be firmly seated against the outer shell. An axial load of 50 tons was applied to the muzzle end to verify the seating of the liner. The muzzle end of the liner shortened by one-sixteenth of an inch; however, the upstream end did not move. The deformation remained locked in upon removal of the load.

Relative movement between the liner and tube was detected when the launch tube was placed in service. Measurements of the liner position relative to the outer shell made after each of the first three firings and after the sixth and eighth are

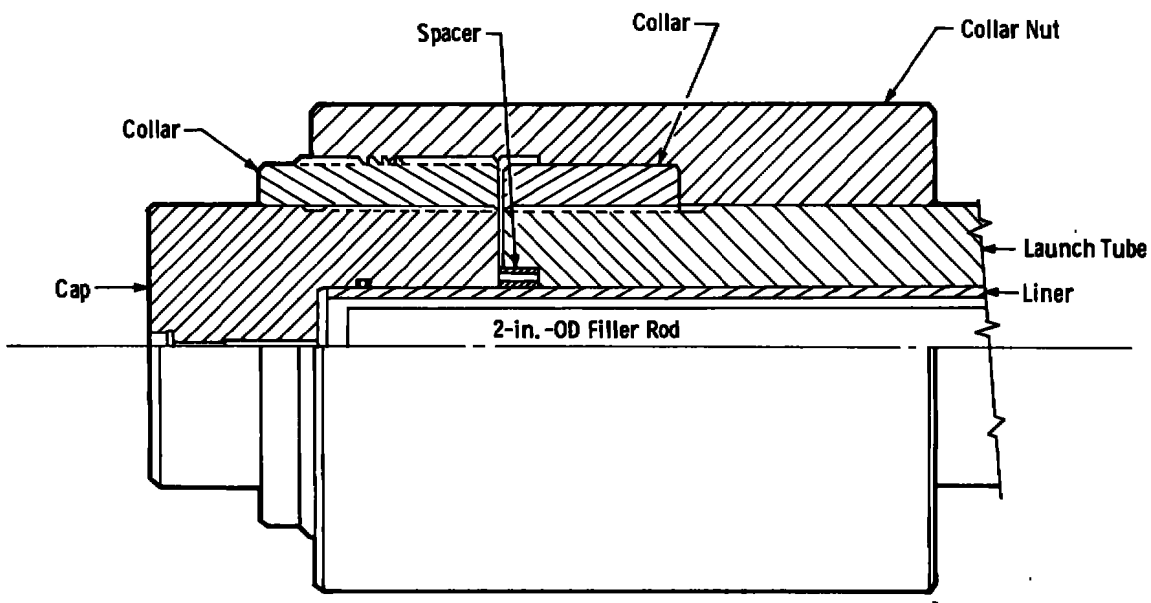


**Figure 1. Upstream end closure for overstraining a relined 7-in.-OD launch tube.**

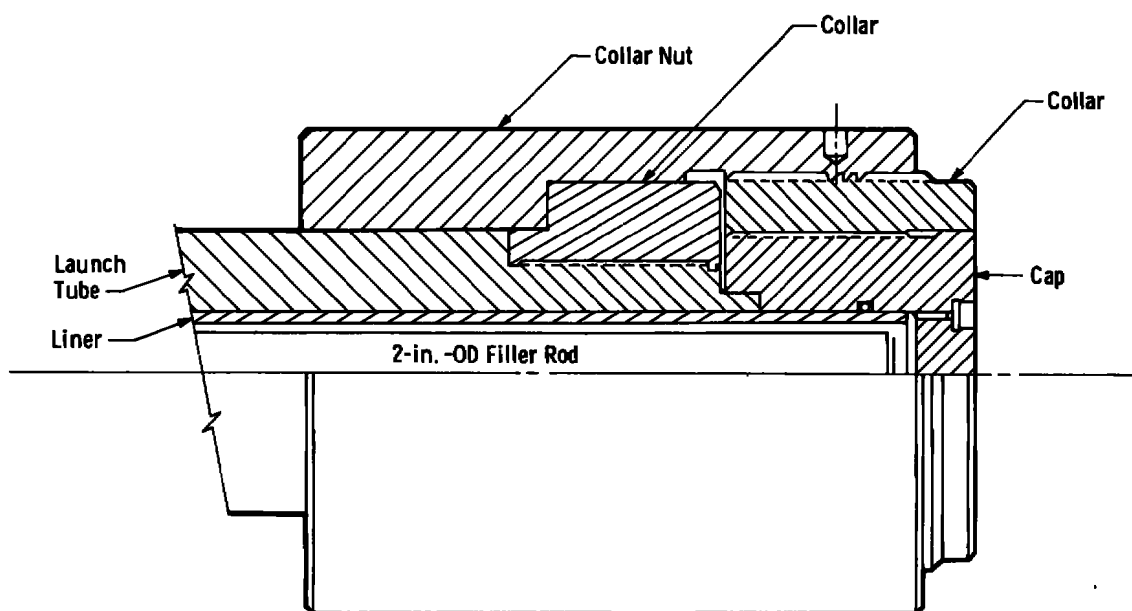


**Figure 2. Muzzle end closure for overstraining a relined 7-in.-OD launch tube.**

shown in Table 1. The conclusion reached at the time was that the movement resulted from relaxation of the stresses locked in as a result of the 50-ton test load.

The experience with this first tube led to the recommendation that the thin film of oil on the liner OD and the axial test load be omitted from future tubes. The oil was not needed for liner insertion and may have contributed to the movement problem.

A 5.5-in.-OD launch tube (SN 011) was also relined with essentially the same setup as Figs. 1 and 2. The assembly was pressurized to 53,000 psi and held for about eight hours. Again, the 53,000 psi was several times the full-wall yield pressure for the liner and just below the yield pressure for the outer shell. An axial test load was not applied to this launch tube; however, movement of the liner occurred during firing. Measurements made after several shots are shown in Table 2. These measurements also reveal that the liner was shortening in length. This could possibly be explained as a Poisson's effect contraction resulting from increased plastic flow in the radial direction.

Because of the liner movement experienced with the first two relined tubes, the design was changed when a third (7-in. OD) required relining. A shoulder was incorporated at the upstream end as shown in Fig. 3 to resist sliding in the downstream direction. The high-pressure section butts up against the tube (Fig. 4) and prevents movement upstream. Along with this design change, the specified overstrain pressures were increased to the maximum that could be attained while keeping a safety factor of two on burst of the outer shell even if this value exceeded the yield pressure of the shell. For the 7-in.-OD tube the specified overstrain pressure level was increased to 85,000 psi and to 60,000 psi for the 5.5-in. one.

Seven-in.-OD tubes that incorporate the aforementioned redesign have been placed in service. These tubes have been fired many times, and no movement of the liner has been detected.

An interesting development did occur during the overstraining of the redesigned lined launch tube as shown in Figs. 2 and 3. Upon initial pressurization, the muzzle end "O" ring seal would leak at about 15,000 to 18,000 psi. This problem had not occurred with the version shown in Figs. 1 and 2. Upon reflection, it was realized that Poisson's ratio effect due to the radial growth under pressure and the end load of the pressure was causing the liner

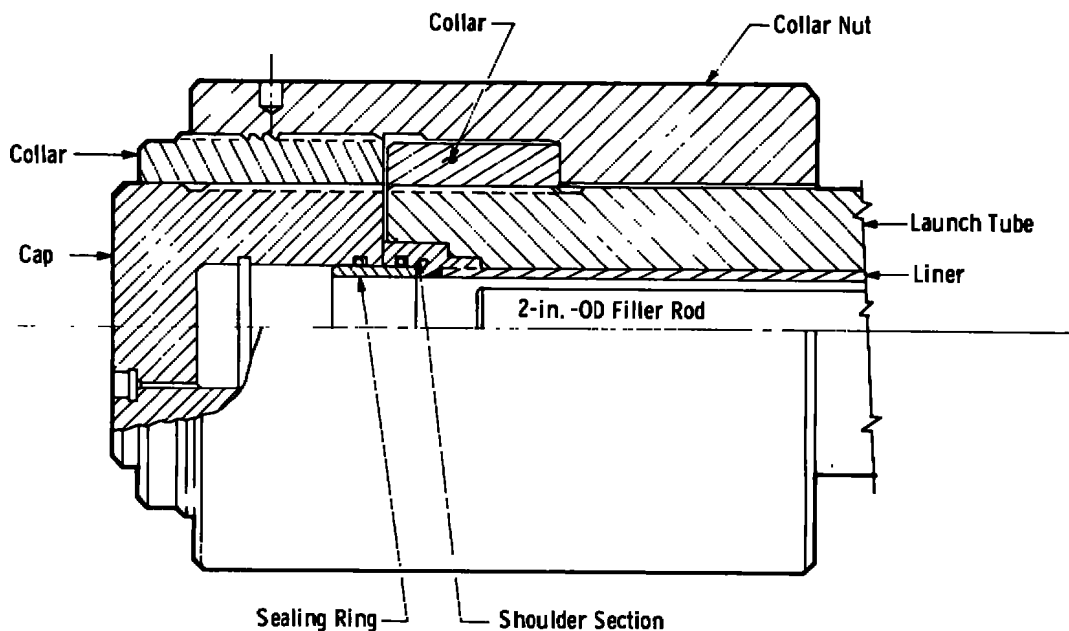


**Figure 3. Upstream end closure for overstraining the modified version of the 7-in.-OD relined launch tube.**

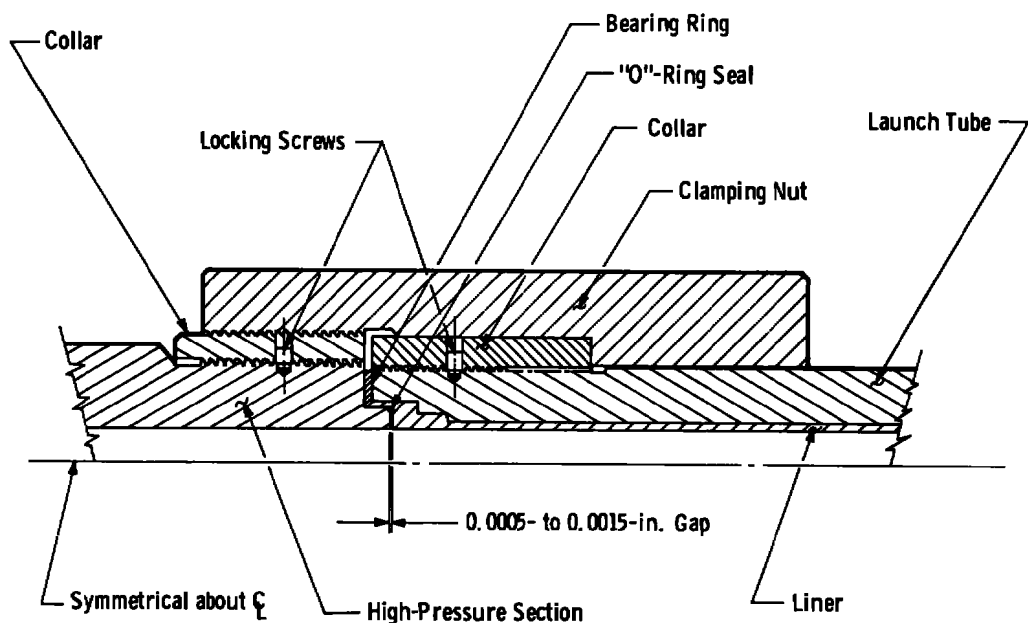


**Figure 4. High-pressure section to launch tube joint.**

to shorten past the seal. Evidently, the "free floating" version of Figs. 1 and 2 shortened from both ends and the liner never slipped past the seals. Also, the liner used in this case was slightly shorter than those used in previous tubes.

Another interesting observation was made during the overstraining procedure. After a pressure of about 35,000 psi had been applied to the configuration of Figs. 2 and 3, the muzzle end was disassembled and it was noted that the liner had permanently shortened. The exact amount of the shortening could not be determined because the protruded length of the liner was not measured prior to the test. The axial stress resulting from the pressure acting on the end of the liner was below the material yield strength; thus, the shortening must have occurred as a result of the swelling of the liner as it closed the radial gap between it and the shell. The tube was reassembled and pressurized to 74,000 psi (the specified 85,000 psi could not be applied due to a limit on the available pressure gage) as shown in Fig. 5. On disassembly it was noted that the liner had lengthened by about 5/8 in. during the cycle. The high pressures involved must have caused the liner to extrude in the axial direction. These results are a clear indication of the severe plastic deformation imposed on the liner material.

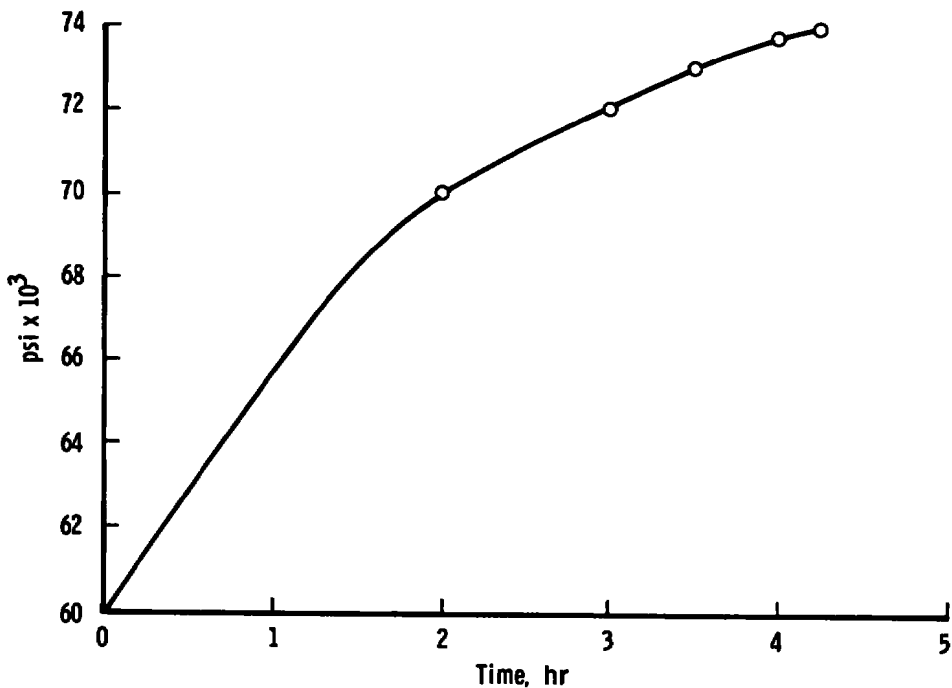


Figure 5. Pressure time trace for relined launch tube (serial No. 018).

### 3.0 AUTOFRETTAGE TEST ARTICLE DESCRIPTION

The typical autofrettage assembly for relining the 35-ft-long launch tubes illustrated in Figs. 1 and 2 shows coupling nuts screwed to the outside diameter of the launch tube. Theoretically, the end effects resulting from the coupling joint will extend as much as 1.5 diameters from the joint. This means that for a 7-in.-OD tube, a 2- to 3-ft length of tube would have to be tested to obtain a central portion free from end effects. Thus, due to these end effects, the required cumbersome handling of many nuts, and the high cost of launch tube material, it was decided to use the much simpler design shown in Fig. 6. The radial dimensions and tolerances of the test article were specified identical to those in the actual autofrettage assembly. The seals were designed to allow for axial growth of the center stud and to seal as close to the ends of the liner as practical. Note that the axial compressive end load present on the liner for the actual autofrettage assembly has been eliminated for the test rig. This small difference was made to reduce the length of the test hardware and material costs. The test hardware should yield results that are conservative as demonstrated in Appendix A, Section A-5. That is, the test article should

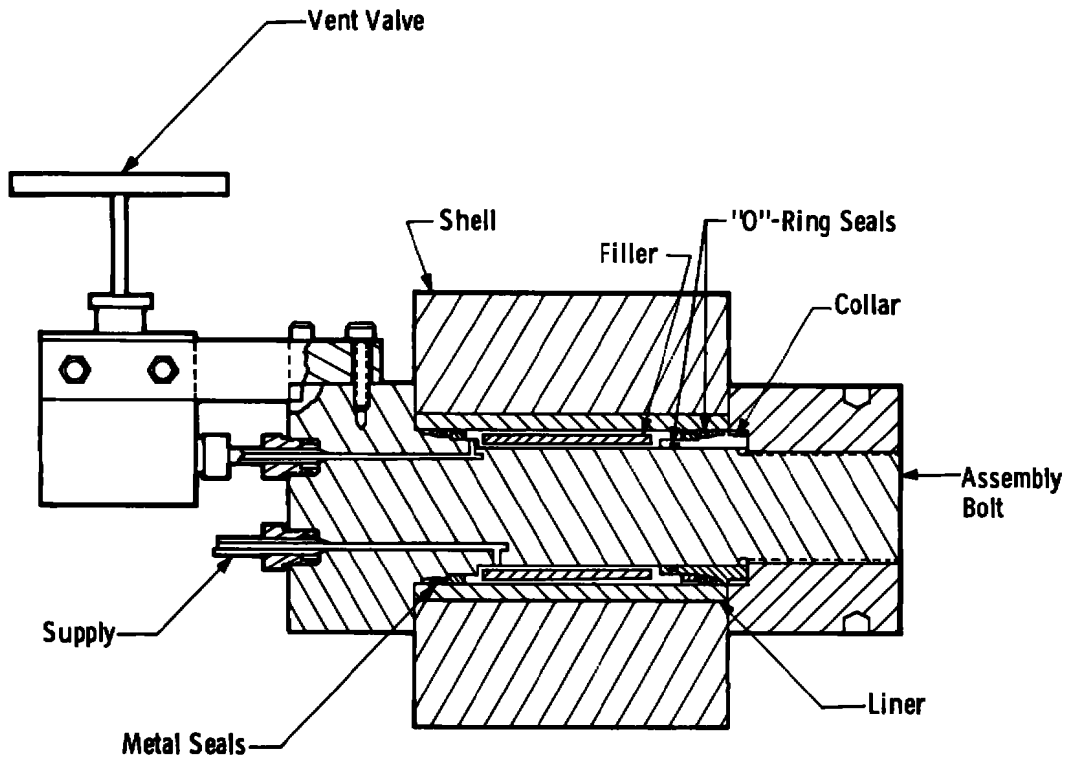


Figure 6. Assembly of test article.

require slightly higher pressures to induce as much interference between the liner and the launch tube as would the actual autofrettage assembly.

The test article outer shells were of the same material as the actual launch tubes (National Forge NA 14 alloy with  $\sigma_{ult} = 159,000$  psi and  $\sigma_{yld} = 145,000$  psi). The liners for the test article were also of the same material as the actual liners (extruded 1026 carbon steel with  $\sigma_{ult} = 85,000$  psi and the  $\sigma_{yld} = 75,000$  psi).

The test article was pressurized by supplying hydraulic fluid through the inlet port of the assembly bolt (Fig. 6). The low-pressure O-ring seals were designed to slide along the assembly bolt and collar and apply load on the high-pressure beryllium copper tapered ring seals. The tapered ring seals were designed to expand and slide out on the tapered surfaces staying in contact with the yielding liner. At high-pressure levels the O-ring rubber seals probably leaked and the metal seals actually became the primary seals for the system. The seal design was somewhat unique in that the seal had to maintain contact even though the liner ID was expanding as much as 0.038 in. and the center stud lengthening 0.077 in. The seal provided good service up to 75,000 psi, and all of the parts were reusable several times.

Two sets of strain gages were mounted on the outer surface of the outer shell diametrically opposite each other to monitor circumferential and longitudinal strain of the outer shell.

## 4.0 DESCRIPTION OF TEST PROCEDURE AND EQUIPMENT

### 4.1 EQUIPMENT

The object of the test was to supply a known pressure to the test article (simulated relined launch tube) and measure the test article's response. Pressure was supplied by a hydraulic pressure intensifier (deadweight tester) and measured using a Heise pressure gage (Figs. 7 and 8). The gage used was temperature compensated and had a scale range from 0 to 100,000 psi. The gage was last calibrated in November 1973.

Response of the test article to the pressure was determined using strain gages mounted on the outer shell. There were two sets of gages diametrically opposite each other so that a check on the validity of the data could be made. Each set consisted of one gage mounted longitudinally and one

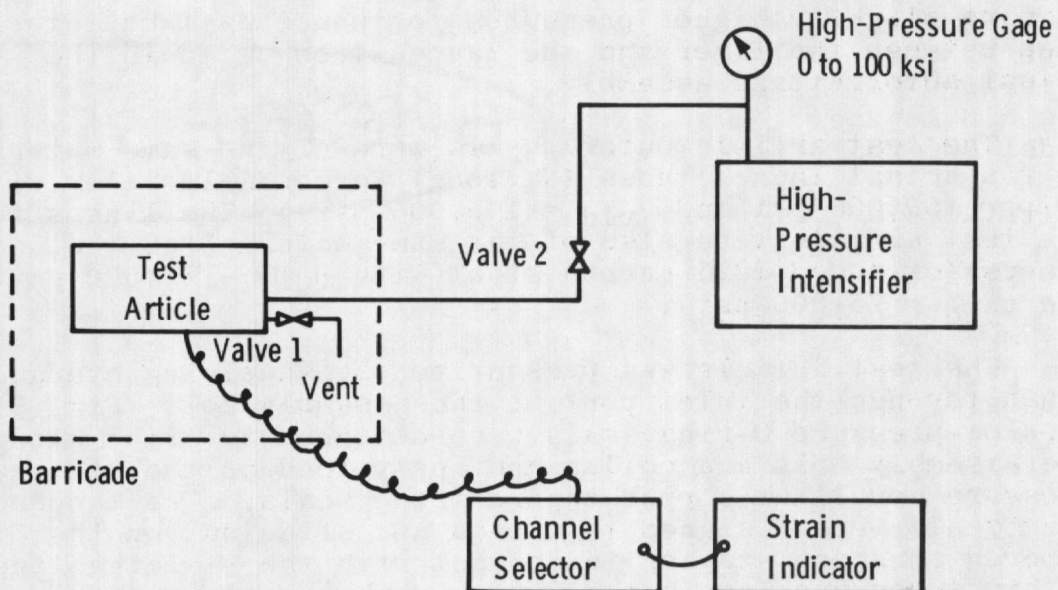


Figure 7. Schematic of test setup.

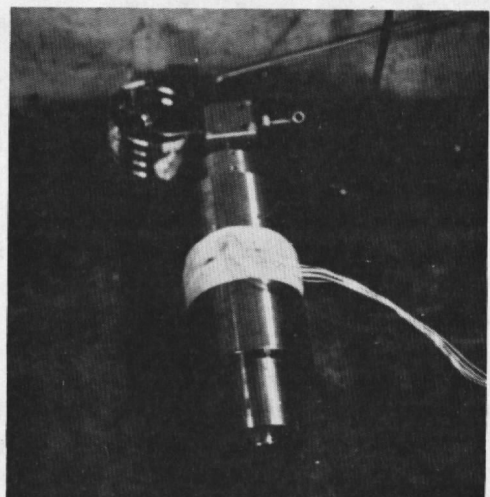
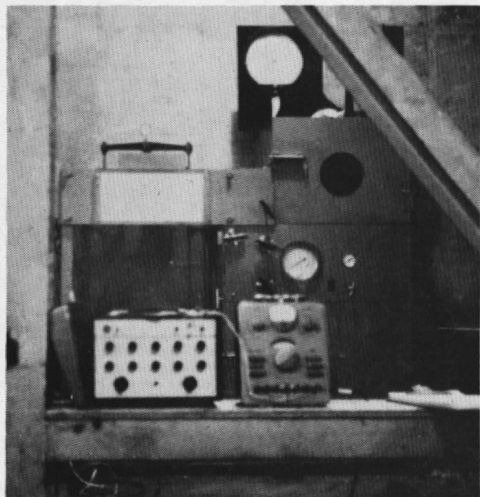


Figure 8. Photographs of test setup.

circumferentially. These gages were of the foil electric resistance type with a gage factor of 2.02, gage length of 0.2 in., and gage resistance of 120 ohms. The gages were bonded to the outer shell using an epoxy cement and cured at room temperature for 24 hours.

Strain readings were taken on an SR-4 Strain Indicator, type N, made by Baldwin, Lima, and Hamilton. Since there were four gages to monitor, a switching unit was used and it was a Baldwin, Lima, Hamilton Switching and Balancing unit, Model No. 225.

#### 4.2 PROCEDURE

The test procedure varied somewhat for each test but had the same basic equipment operation procedure. It is assumed that the reader is familiar or can readily obtain the procedure for operating a commercial hydraulic pressure intensifier and no details of that phase of operation will be presented here. Thus, the basic operating procedure was as follows: (Ref. Fig. 7)

1. The test article was assembled and attached to the high-pressure line.
2. Air was expelled from the system by opening vent valve 1 and pumping hydraulic fluid through the test article until fluid ran steadily out of the vent line.
3. Vent valve 1 was closed and the test article charged to the desired pressure.
4. Once desired pressure was reached, the charging unit was stopped and the indicated strain from the four strain gages was read and recorded. At this point, the pressure could be maintained by closing valve 2, vented by opening valve 1, or increased by additional pumping with the intensifier.
5. Strain-gage readings were taken at various pressure levels until the maximum desired level was achieved. Gage readings were also recorded at approximately the same levels as the pressure was decreased. Strain-gage readings were also recorded at "0" pressure so that residual effects could be examined. This completed the first cycle and additional cycles could be made by repeating steps 1 through 5.
6. After all testing criteria had been met, the test article was disassembled and the shell and liner assembly measured to obtain the outside diameter of the shell, length of the shell, inside diameter of the liner, and length of the liner.

7. The shell and liner assembly was then tested to verify that the liner had plastically yielded and developed a tight interference fit with the outer shell. To do this, an axial force was applied to the liner while holding the shell. (The axial-force resistance should be proportional to the interference induced by the autofrettage method.) The test was performed by a Baldwin Universal Testing Machine with maximum capability of 120 kips. The load monitor device was a Tate-Emery Load Indicator with an accuracy of  $\pm 1$  percent and calibrated annually.

Some of the liners were pushed out by the above-mentioned method, and their dimensions measured to correlate the amount of interference measured with the strain-gage readings of residual stress. The results of this procedure are presented in Sect. 8.1.

#### 4.3 SELECTION OF MAXIMUM AUTOFRETTAGE PRESSURE

As previously discussed, the first efforts at autofrettaging liners into the actual launch tubes were based on applying a pressure of 50,000 psi to the assembly. The 50,000 psi was arbitrarily chosen as a value below bore yield of the outer shell and sufficiently higher than full-wall yield of the liner. Subsequent tests demonstrated this pressure to be insufficient, and the overstrain pressures were increased to the maximum that could be attained while keeping a safety factor of two on burst of the outer shell. Burst of the outer shell was calculated as if the pressure applied to the liner was transmitted undiminished to the outer shell.

For safety reasons, the pressures used in the autofrettage tests described in this report were also limited by requiring a safety factor of two on burst of the outer shell as determined from the strain-gage readings during the tests. In practice, the tests actually were limited to about 90,000 psi because of difficulty with the seals and the pressure rating of the tubing used to plumb the rig. The tubing was rated for 100,000 psi; however, the safety factor was deemed marginal at that pressure. Also, the seals tended to leak above 75,000 psi and 80,000 to 90,000 psi seemed to be about the maximum attainable without appreciable difficulty.

#### 4.4 ORIGINAL DIMENSIONS OF THE TEST PIECES

The original dimensions of the various test pieces are tabulated in Table 3. Note that liners were machined with

three different nominal outside diameters: 2.990, 2.982, and 2.976 in. The midrange or medium clearance (0.020 in.) liner with a 7-in.-OD shell was chosen as the reference or baseline test. All tests were performed with this combination except when effects of liner clearance or outer shell thickness were being determined.

#### 4.5 INTERPRETATION OF STRAIN-GAGE READINGS

Two sets of strain gages were mounted on the outside diameter of the outer shell. Each set consisted of one circumferential and one axially oriented gage. During a test, the pressure was applied to the liner inside the shell; hence, the gages recorded only the strain resulting from contact between the liner and outer shell. No strain was, or should have been, recorded as long as a clearance gap existed between the two. Upon removal of the applied pressure, any strain recorded could be attributed to plastic growth of the liner with a resulting interference created between the liner and outer shell.

### 5.0 DISCUSSION OF TEST RESULTS

#### 5.1 EFFECT OF PRESSURE-HOLDING TIME

The first test performed in this experiment involved the holding time variable. The test plan was to pressurize to a predetermined level, hold for a long period of time, and monitor the strain-gage readings. Table 4 shows the effect of hold times up to five hours with pressures up to 50,000 psi for a medium-clearance (0.020 in.) liner. The data are plotted in Fig. 9 as a function of time. Note that in one case there was a slight drift downward in strain reading, whereas in the other case the gage readings drifted upward. In neither case did the gage readings change by more than ten percent, and the variations noted are probably attributable to drift of the instrumentation.

The original test plan was to pressurize this liner to 75,000 psi and hold for a long time; however, seal leaks developed and the pressure was held only momentarily. The test rig was then disassembled and no further tests performed. Experience gained in later tests showed that the seals characteristically leaked the first time 75,000-psi pressure was applied but would hold if the pressure was immediately re-applied.

Further evidence that pressure hold time has little effect, if any, can be seen in Table 5. The primary objective of the test for the data tabulated in Table 5 was

different; however, hold times of 5 to 15 minutes at pressure were common. Several times during the test, various pressure levels were held with no time effect noted. Note in particular that a pressure of 73,000 to 75,000 psi was held for about 40 minutes toward the end of the test with negligible drift in gage readings.

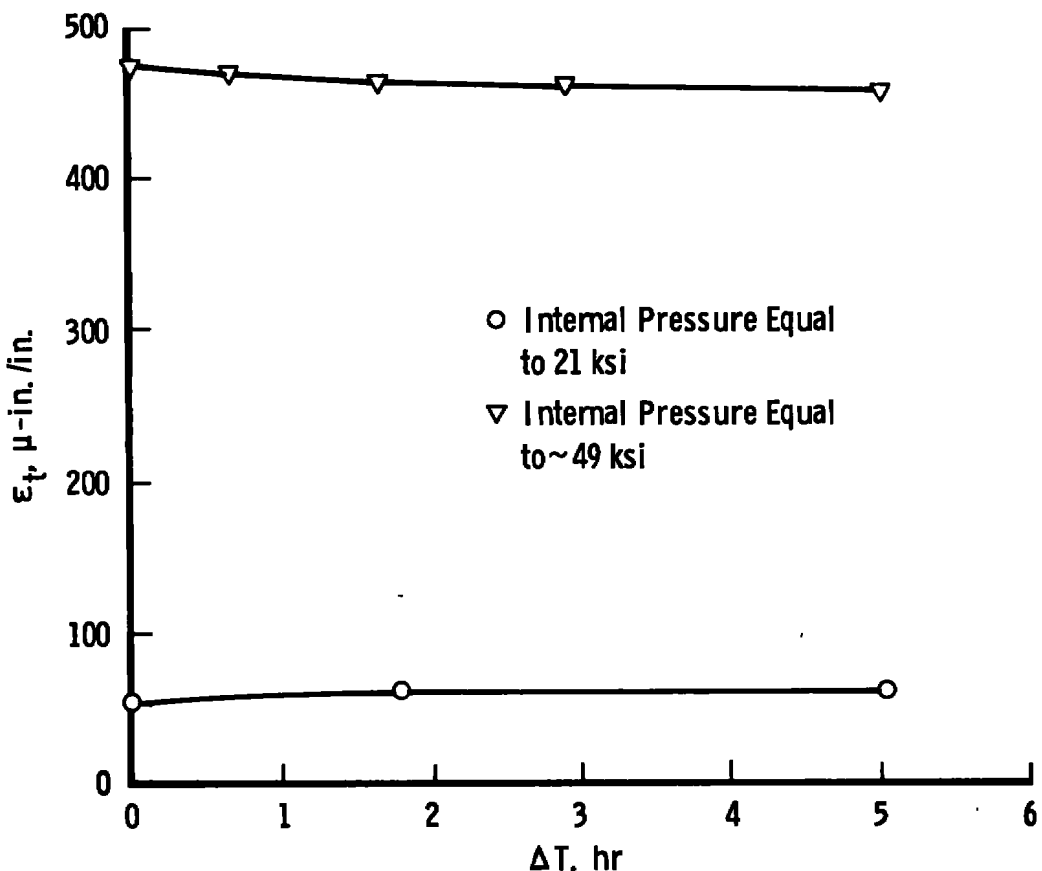


Figure 9. Circumferential strain at the OD of a 7-in. shell as a function of time using a medium-fit (0.020-in. clearance) liner.

## 5.2 EFFECT OF PRESSURE CYCLING

Pressure cycling effects were primarily evaluated in Test 2 but can be verified to some extent in all the tests. Test 2 experimental data, tabulated in Table 5, show that multiple cycles to any pressure level, provided the pressure has not exceeded that level, result in essentially the same strain-gage readings for each cycle. This lack of any cyclic effect is shown graphically in Fig. 10, which is based on the Table 5 data.

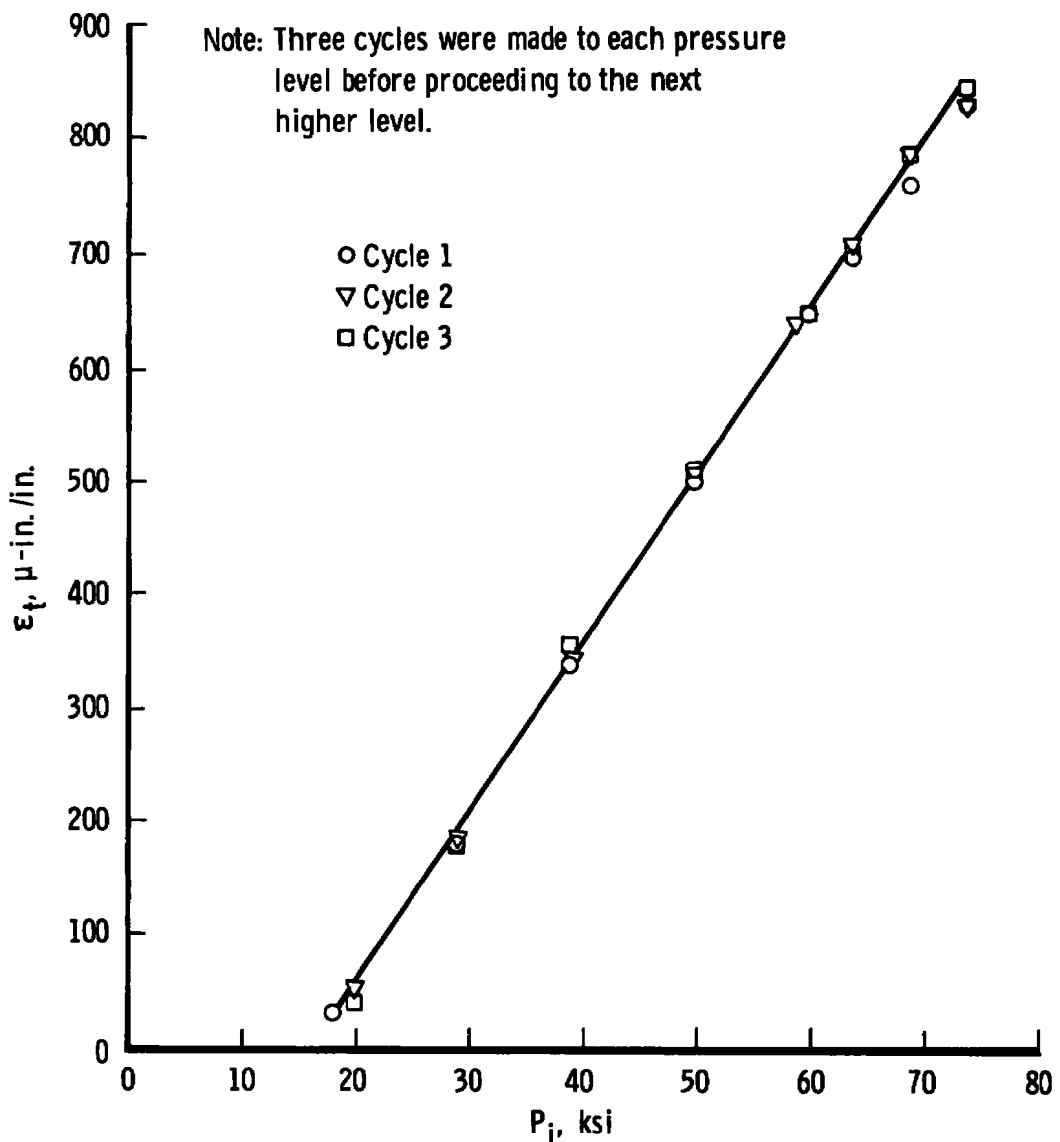


Figure 10. Circumferential strain at the OD of a 7-in.-OD shell as a function of internal pressure using a medium-fit (0.020-in. clearance) liner.

The Table 5 data also show that once a pressure level was exceeded, the strain-gage readings differ from the values taken prior to exceeding that pressure. The shift is generally more than the "locked-in" strain (strain at "0" psi) can account for. The indication is that the material is subject to appreciable strain hardening.

### 5.3 EFFECT OF LINER CLEARANCE

The effect of liner clearance was investigated using a 7-in.-OD shell with three different clearance liners. The three diametrical clearances were nominally 0.011, 0.020, and 0.025 in. The clearances are referred to in the following as tight, medium, and loose fit.

Tables 5 and 6 contain data obtained with medium-fit liners. Table 5 shows a residual circumferential strain of 77 and a longitudinal strain of 5  $\mu\text{in./in.}$  after a maximum applied pressure of 75,000 psi. For Table 6, the maximum applied pressure was 74,000 psi and the residual strains read immediately after venting the pressure were 80 and -9.0  $\mu\text{in./in.}$  for circumferential and longitudinal, respectively.

Data for two tight-fit liners are shown in Tables 7 and 8. Table 7 shows that residual strains of 78 and 20  $\mu\text{in./in.}$  circumferentially and longitudinally, respectively, result from an applied pressure of 75,000 psi. The corresponding strains from Table 8 are 69 and 10  $\mu\text{in./in.}$ . These data are considered to be essentially in agreement with the previous data cited for the medium-fit liners. The two-to-one variation in the longitudinal strain between the two tight-fit liner tests is probably indicative of equipment drift or slight differences in frictional forces between the liners and the shell.

Data obtained for two loose-fit liners are shown in Tables 9 and 10. Residual strains for these varied from 45 to 51.0  $\mu\text{in./in.}$  in the circumferential direction and 9 to 12  $\mu\text{in./in.}$  in the longitudinal after application of 75,000-psi pressure.

The medium- and tight-fit liners produced essentially the same residual strain (or interference fit with the outer shell); however, the loose-fit liners produced less. Tables 9 and 10 for the loose-fit liners show that the circumferential strain measured at 75,000-psi pressure varied from about 781 to 830  $\mu\text{in./in.}$ . An almost identical spread is shown in Tables 7 and 8 for the tight-fit liner; hence, both loose- and tight-fit liners exert the same pressure against the outer shell with the test rig under pressure. The only obvious explanation for the difference in residual strains is that some additional spring-back resulted from the additional plastic flow required for loose-fitting liners.

The trend appears to be that liners can be too loose for effective seating against the launch tubes during

autofrettaging; however, the apparent difference in residual strains noted for the loose liner should not be accepted as completely conclusive. The logical trend would be that the liner producing the largest residual circumferential strain should also produce the largest residual longitudinal strain. Yet the medium-fit liners resulted in more circumferential but less longitudinal strain than did the loose liners. The point is that equipment error due to drift and temperature changes could easily result in 10 to 20  $\mu\text{in./in.}$  of strain error. On several of the tests, the strain gages were monitored for several minutes following completion of the test. Drifts of 10 to 15  $\mu\text{in./in.}$  were noted, see Tables 5 through 10. In most cases, the change in gage readings indicated increased contact stress on the outer shell. Logically, if any stress change occurred, one would expect a lowering of outer shell stress caused by relaxation of the liner. Consequently, the relatively small differences in residual strains measured can be subject to question.

#### 5.4 EFFECT OF PRESSURE LEVEL

The residual interference between liner and shell produced by various pressure levels was studied using the 7-in.-OD shell and a medium-fit liner. Table 5 contains this data. The procedure followed was to pressurize the test rig to a particular level, vent the pressure, record the residual strain, and then proceed to the next higher level. Note that no residual strain was produced until the applied pressure had exceeded 50,000 psi. (After the first cycle to 20,000 psi, a residual compressive strain of 10  $\mu\text{in./in.}$  was measured. This is obviously physically impossible and should be attributed to equipment drift.) After a pressure of 60,000 psi was applied, a residual circumferential strain of 25 to 28  $\mu\text{in./in.}$  was measured. Figure 11 shows the measured residual strains for the various pressures up to the maximum applied of 77,000 psi. Data extracted from some of the other tests are also plotted in Fig. 11. The highest residual strain measured (77  $\mu\text{in./in.}$ ) corresponds to a calculated contact pressure between the liner and shell of 5,125 psi. To test the frictional resistance developed, an axial force was applied to the liner while holding the shell and it took 100,000 pounds to cause any movement. A second 7-in. shell with the loose-fit liner was tested, and movement occurred at about 120,000 pounds. A third (tight-fit liner) and a fourth (medium-fit liner) were tested and no movement could be produced when the testing machine reached its maximum capacity of 120,000 pounds. In terms of the 35-ft-long launch tubes, these values would extrapolate to over  $4 \times 10^6$  pounds of holding force for the liner. This

value was considered more than adequate. In addition, previous launch tubes had been autofrettaged to 75,000 psi and demonstrated satisfactory performance when placed in service. The conclusion was that 75,000-psi pressure is adequate for 7-in.-OD launch tubes.

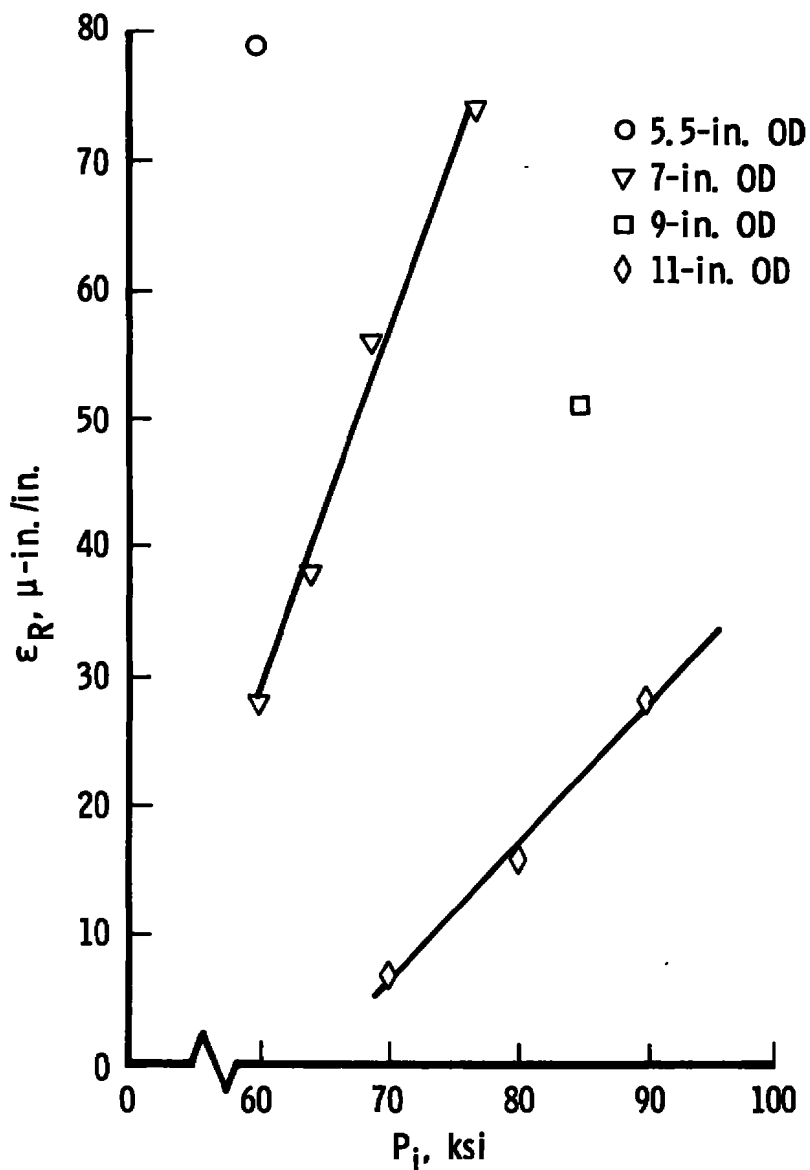


Figure 11. Residual strain as a function of internal pressure.

## 5.5 EFFECT OF LAUNCH TUBE OUTSIDE DIAMETER

Tests were performed on outer shells varying from 5.5- to 11-in. OD. The object was to try to determine the pressure that must be applied to develop the same residual contact pressure of 5,125 psi found to be adequate for the 7-in.-OD launch tubes. For the various shells, the following residual strains would have to be produced:

<u>Shell OD</u>	<u>Residual Strain, μin./in.</u>
5.5	145
7.0	77
9.0	43
11.0	28

The tests involving the 5.5-in. outer shell with a medium-clearance liner were limited to 60,000 psi for safety considerations. The residual strain produced is shown in Table 11 to be 79 μin./in. Since this value was below the anticipated requirement, an axial load was also applied to it and relative movement occurred at about 102,000 pounds. This means a lower contact pressure produced the same frictional resistance as noted previously for at least one of the 7-in.-OD shells. The reason for the discrepancy is not known. The 5.5-in. shell was machined from a 7-in. shell after the 7-in. testing was completed and perhaps slight differences in surface finishes existed, although the bore of the shell was not remachined.

A 9-in.-OD shell with a medium-clearance liner was tested to 85,000 psi as a guess at the required pressure, and a residual strain of 50 to 55 μin./in. resulted, see Table 12. This proved slightly in excess of the anticipated requirement. An axial load was also applied to the liner, and no movement could be detected when the machine maximum capacity of 120,000 was reached.

An 11-in.-OD shell with a medium-clearance liner was tested to 90,000 psi. A residual strain of 28 μin./in. was recorded, see Table 13. This value matched the anticipated requirement. An axial load was also applied to this liner, and relative movement occurred at about 110,000 pounds.

On the basis of the above results, a plot was constructed to relate the required autofrettage pressure versus the launch tube outside diameter. Figure 12 shows this variation.

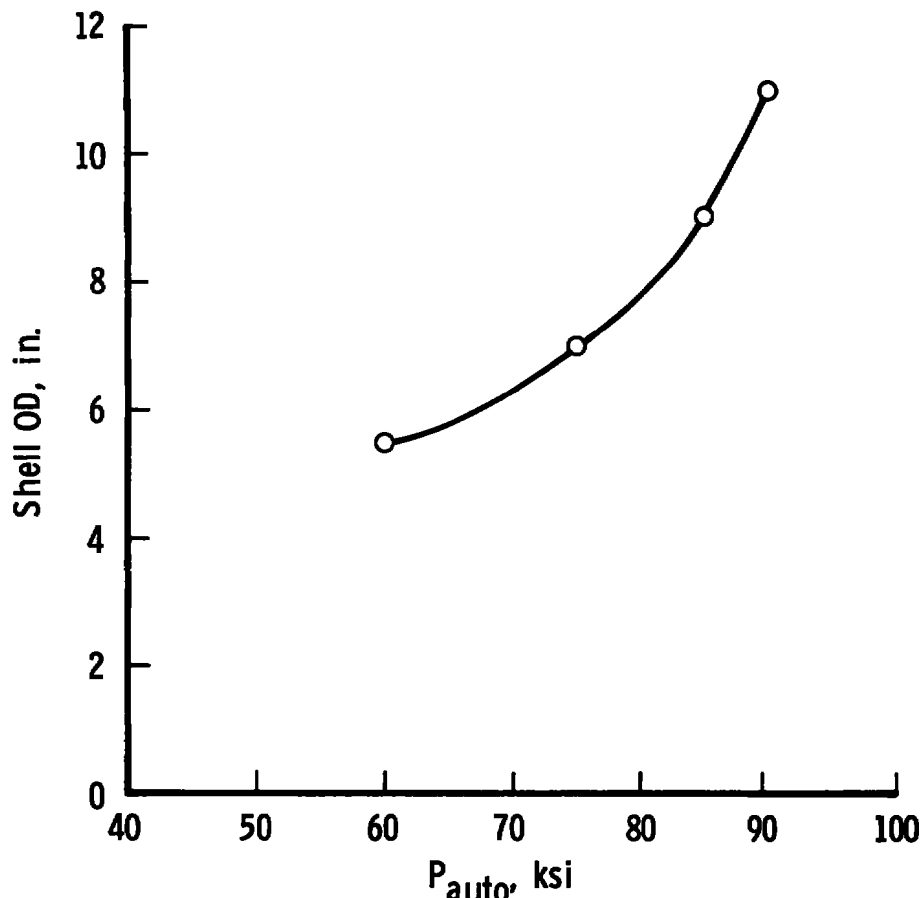


Figure 12. Required autofrettage pressure for any size shell with a 3-in. ID.

## 6.0 PREDICTION OF THE HOLDING FORCE PRODUCED BY AUTOFRETTAGING

As discussed in the previous section, many of the liner-shell combinations were tested after autofrettaging to determine the force required to move the liner relative to the shell. The forces measured are shown in Fig. 13 by the various symbols as a function of the measured residual strain for that liner-shell combination. For comparison purposes, a theoretical axial force was also calculated as a function of strain. The equation for the theoretical axial force comes from two basic equations:

$$F = \mu N \quad (7)$$

and

$$N = 2 \pi a \ell P_c \quad (8)$$

where

$F$  = frictional force, lb  
 $\mu$  = coefficient of friction  
 $N$  = force perpendicular to the  
 sliding surfaces, lb  
 $a$  = inside radius of shell, in.  
 $\ell$  = length of the liner, in.

and

$P_c$  = contact pressure between the liner and shell, psi

This contact pressure is shown in Appendix B to be related to the measured strain by the equation:

$$P_c = \frac{E \epsilon_t (K^2 - 1)}{2} \quad (9)$$

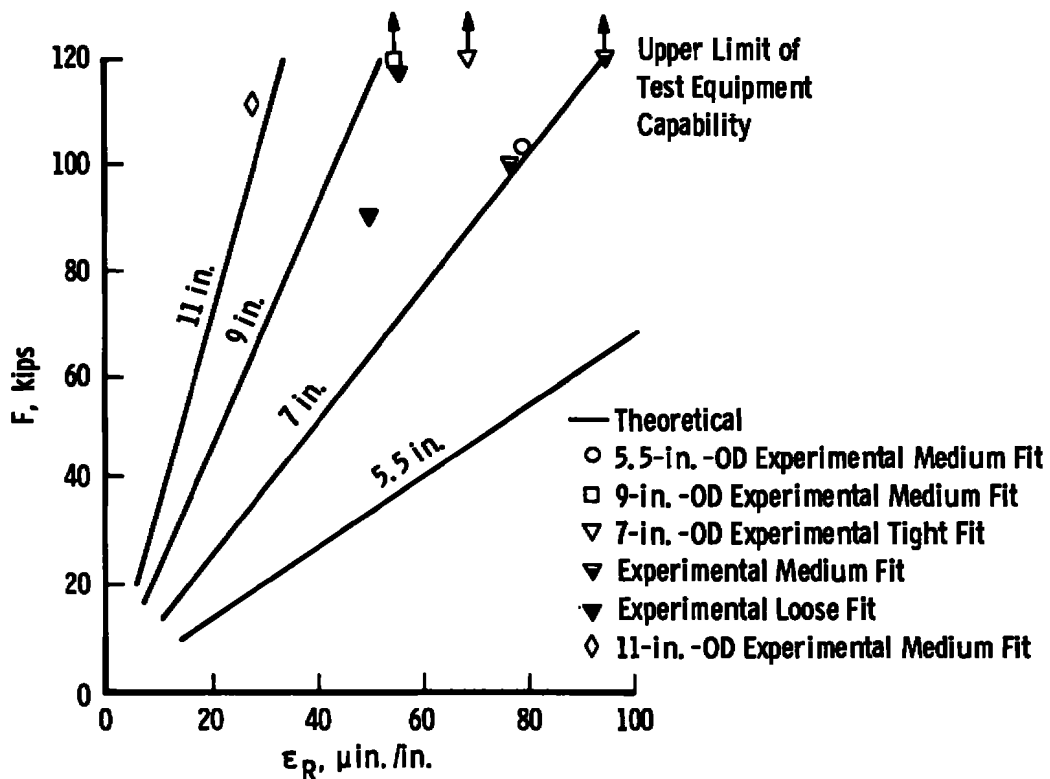


Figure 13. Comparison of theoretical to experimental axial force.

thus, substitution of Eqs. (8) and (9) into Eq. (7) yields

$$F = 6 \pi \ell a \epsilon_t (K^2 - 1) (10^6) \quad (10)$$

for  $E = 30 \times 10^6$  and  $\mu = 0.2$ . Equation (10) is plotted to obtain the theoretical curves in Fig. 13.

The experimental data show no definite pattern except that the axial force measured was always higher than that theoretically calculated. The friction coefficient could, of course, be a source of error in the theoretical curves.

## 7.0 COMPARISON OF EXPERIMENTAL RESULTS WITH THEORY

As was mentioned previously, the initial attempts at autofrettaging liners into launch tubes failed. A pressure of 50,000 psi was applied to a 7-in.-OD launch tube with a medium-clearance liner. The 50,000-psi pressure was calculated to be three to four times greater than the pressure required for full-wall yield of the liner. The idea was that the liner would plastically flow until contact was made with the outer shell. It was further believed that the pressure would then be transmitted almost undiminished to the outer shell causing it to grow elastically. The elastic growth of the outer shell would permit additional plastic growth of the liner and result in an interference fit between the liner and shell upon release of the pressure. Unfortunately, things did not go exactly as anticipated. The liners evidently had an elastic spring-back large enough to offset the anticipated interference.

The initial failure of the autofrettage procedures to adequately seat the liners caused some concern that the theoretical equations were in gross error. The same basic theory is frequently used in design of high-pressure sections, powder chambers, and pump tubes for the Hyperballistic Range (G). Thus, a verification of the theory was also made a part of this program.

The equations used in component design are shown in Appendix A. The launch tubes during the autofrettage procedure are calculated as closed-end pressure vessels (Fig. 1). The liner is assumed to be an open-end pressure vessel with an applied end load. For the test setup (Fig. 6), the outer shell can best be modeled as an open-end pressure vessel without axial load. The liner for the test rig is assumed to be an open-end vessel without an end load until contact

with the outer shell. After contact, the liner is analyzed as an open-end pressure vessel with an internal and external pressure.

For the test article, Eq. (A-47) shows that the liner should be completely plastic (full-wall yield) at a pressure of 14,300 psi. Table 5 data show that contact between the shell and liner had occurred at 18,000 psi for a medium-fit liner. In general, it was noted during the various tests that the strain gages indicated contact between liner and outer shell at pressures slightly above 15,000 psi. This correlation indicates reasonable agreement between theory and actual behavior.

As a further check, Eq. (A-55) was compared with the experimental data. Equation (A-55) supposedly related the theoretical external pressure ( $P_o$ ) to the applied internal pressure ( $P_i$ ) for plastic equilibrium of an open-end pressure vessel. Hence, the equation should be appropriate for the liner after contact with the outer shell. The experimentally determined contact pressure,  $P_c$ , was calculated from Eq. (B-3) and the strain-gage readings. This calculated  $P_c$  and the corresponding value of  $P_i$  were then plotted as experimental data in Figs. 14 through 17. (The values plotted are the  $P_c$  resulting from the first cycle to a  $P_i$ . Strain hardening occurs during the first cycle and changes subsequent values.) Equation (A-55) was used to plot the theoretical contact pressure,  $P_o$ , and the results are also shown in the same figures. Note that the theoretical equation in each case overestimated the contact pressure required to balance the applied  $P_i$ . This trend is consistent with one of the basic assumptions in the plasticity theory used in the theoretical development. The assumption is that once the material has been stressed to yield level, yielding will continue under constant load. Most materials will show some strain hardening effects and require an increase in load for continued yielding. The implication of this is that plastic flow does not occur as freely as the theory predicts; hence, not as much load is transferred to the outer shell. Also, the theoretical computations were based on 75,000-psi yield strength. This value was quoted as a typical value by the suppliers of the liners; however, it was not verified. The liners are fabricated from plate rolled into a cylinder, welded, and reduced to size by cold drawing over mandrel to the desired dimensions. The yield strength could conceivably be higher, and a higher yield strength would lower the predicted  $P_o$  values from Eq. (A-55).

Based on the above observations, the theoretical development appears to be slightly conservative but in reasonable agreement with the experimental data.

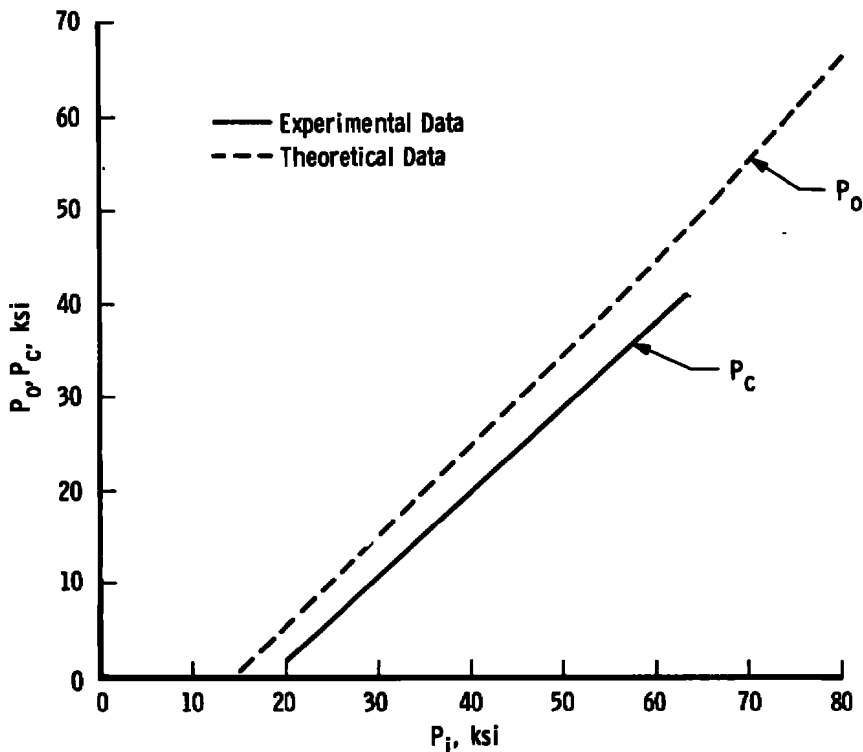


Figure 14. Comparison of theoretical to experimental liner-shell contact pressure for 5.5-in.-OD shell with medium-fit (0.0181-in. clearance) liner.

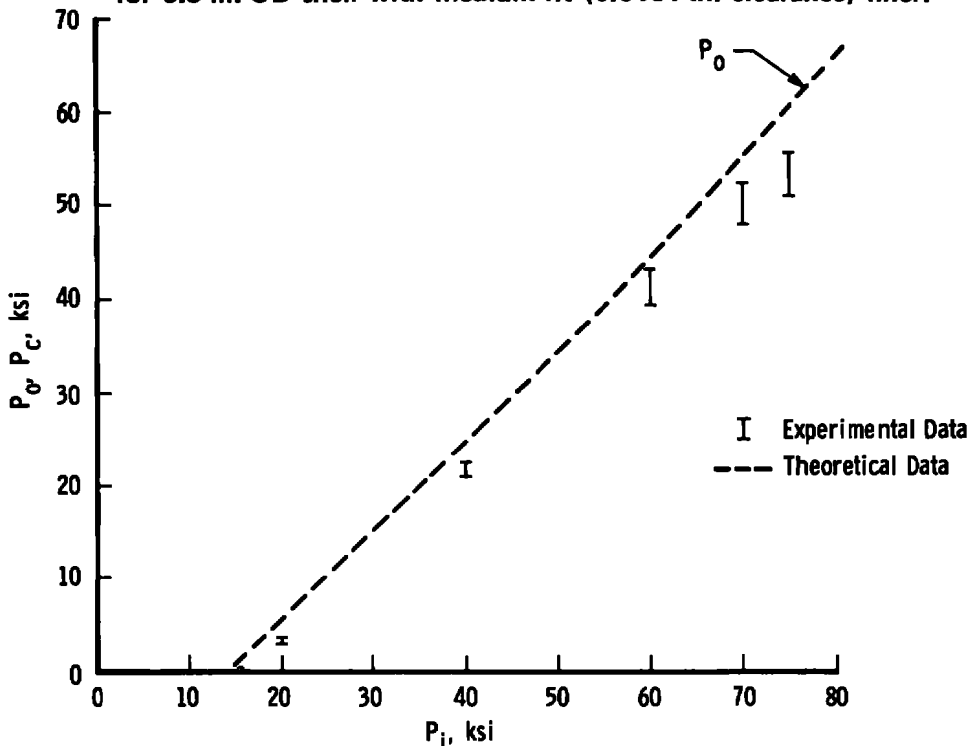


Figure 15. Comparison of theoretical to experimental liner-shell contact pressure for a 7-in.-OD shell with various liners.

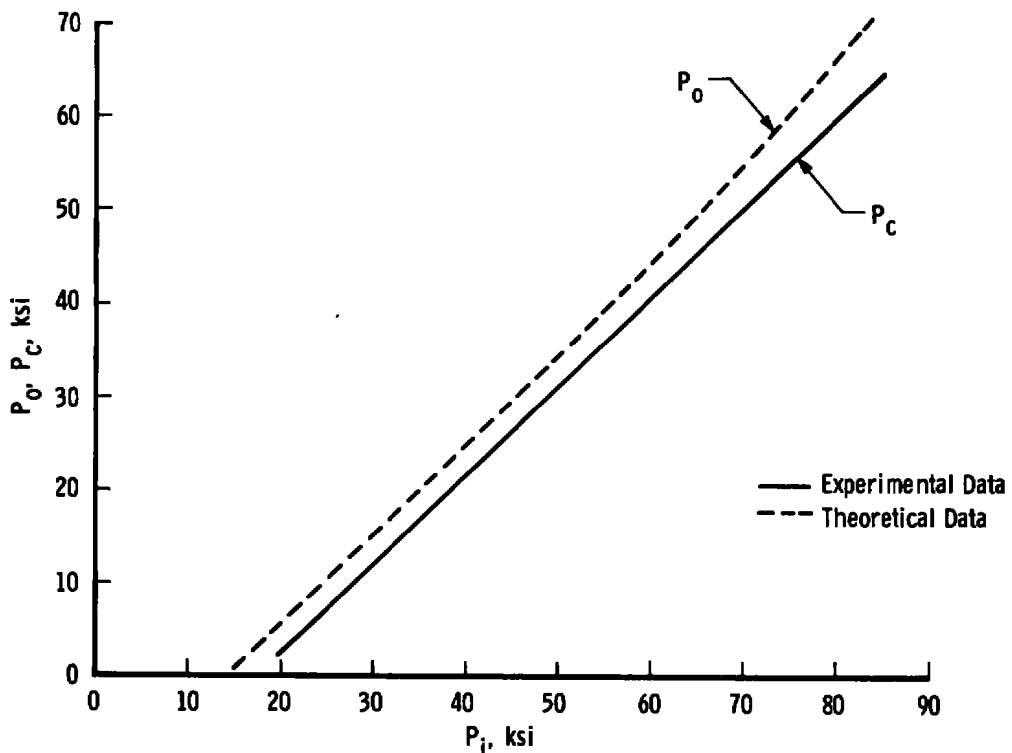


Figure 16. Comparison of theoretical to experimental liner-shell contact pressure for a 9-in.-OD shell with medium-fit (0.0173-in. clearance) liner.

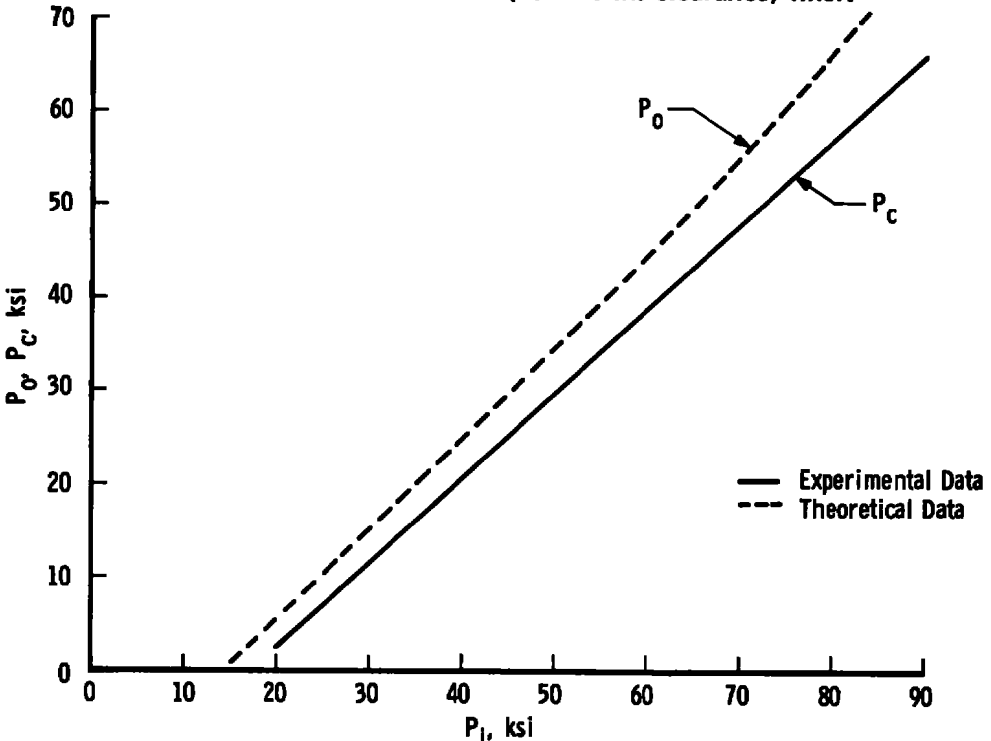


Figure 17. Comparison of theoretical to experimental liner-shell contact pressure for an 11-in.-OD shell with medium-fit (0.0181-in. clearance) liner.

## 8.0 MISCELLANEOUS OBSERVATIONS

### 8.1 DISCREPANCIES IN CONTACT PRESSURE

Three of the liners were completely pushed out of their shell. Final dimensions were taken of both liner and shell and are shown in Table 14. From these measured values, an interference can be determined and a contact pressure calculated using the standard equation for a two-layered pressure vessel, i.e.,

$$p_{c5} = \frac{E 5(d^2 - b^2)(b^2 - a^2)}{2b^3 (d^2 - a^2)}$$

$d$  = radial interference

$a, b$  = inner and outer radius of the liner, respectively

$d$  = outer radius of the shell

The contact pressures calculated from this equation are also shown in Table 14. These values differ from the contact pressure calculated from the measured residual strains using Eq. (B-3). The latter values are also included in Table 14 for comparison purposes.

Intuitively, one would expect the contact pressure based on the residual strain to be larger than that determined from the interference measurements due to the erosion effect of pushing out the liner; however, in all three cases the reverse was true. The only obvious conclusion is that a combination of strain-gage reading error and dimensional measurement error caused the discrepancy. The maximum deviation was 1,148 psi which corresponds to as little as 17.2  $\mu$ in./in. of measured strain or 0.0004 in. of radial interference. The most likely source of error would be a combination of the two.

### 8.2 LINER LENGTH CHANGES

After each of the first three pressure cycles for Test No. 1 (Table 4 data), the test article was disassembled and the liner remeasured. Table 15 shows the dimensions recorded. As expected, the liner dimensions showed clear evidence of plastic flow after each cycle. One of the more interesting dimensional changes was the length. Note that the length shortened 0.019 in. during the first cycle and an additional 0.005 in. during the second. This extrapolates to over 1 in.

of movement when the 35-ft-long launch tubes are autofrettaged. Experience has shown that this much movement must be designed into the seal arrangement.

For the third cycle (pressure increased from 51,000 to 75,000 psi), the liner lengthened by 0.0015 in. over its previous length. Evidently, the Poisson's ratio effect causes an initial shortening; however, the liner finally becomes so plastic it begins to flow along the path of least resistance. This is a clear indication of the severity of the plastic work sustained by the liner.

### 8.3 APPLICATION OF RESULTS TO OTHER LINERS

Previous sections of the report have shown that the theoretical equations are in reasonable agreement with the experimental data. That is, the response of the liner to the applied pressure can be adequately, though conservatively, described by the theory. The fact that the autofrettaging pressures produced less frictional holding forces than expected can be attributed to strain hardening of the material and the resulting elastic spring-back of the liner when the pressure was removed. If this spring-back could be predicted, liner-shell combinations of other dimensions could be autofrettaged on the basis of analytically predicted parameters.

An attempt was made to calculate this spring-back from the data obtained in this experiment. Unfortunately, the spring-back demonstrated by an elasto-plastic liner was so small that the setup used could not accurately measure it. Yet, the effect on the contact pressure is appreciable. For example, 0.0005 in. of radial spring-back relieves about 1,500 psi of the contact pressure for a 7-in.-OD shell. This corresponds to almost one-half of the total contact pressure measured.

### 9.0 CONCLUSIONS

The study conducted showed that hold time at pressure has negligible effect on the residual strains locked in after the pressure is released. This proved true for pressures held as long as five hours. Thus, in future autofrettage procedures, the pressure hold times can be considerably reduced. Nominal hold times of five minutes should be sufficient.

The conclusions regarding liner clearance are not nearly as positive. Liners with diametrical clearances from 0.011 to 0.020 in. responded the same to the autofrettage pressures;

however, two liners with 0.025-in. clearance differed. The liners with the larger clearance appeared to have more spring-back upon release of the pressure. Consequently, future launch tubes should be relined with the tight- to medium-fit liners.

Multiple cycles to the same pressure level were also found to have negligible effect on the residual strains and can be eliminated as a requirement for future relining projects.

As the study progressed, it became apparent that the primary factor influencing the effectiveness of the auto-frettaging procedure was the pressure level achieved. No interference was obtained at pressures below 50,000 psi. The particular amount required was found to be a function of the launch tube OD.

The experimental data verified that the theoretical equations are reasonably accurate. Furthermore, the error in the theory is on the conservative side for the normal design usage. That is, the amount of plastic yielding is slightly overestimated.

Many calculations and plots were made from the experimental data in an effort to predict the performance of a different liner. This would have been very helpful in the future when different size liners might be used. However, our efforts proved unsuccessful, and at this point it would be difficult to theoretically predict accurate results of a liner with different geometry to the ones tested herein.

If desired, a direct verification that interference has been created between the liner and launch tube can be obtained during the autofrettage procedure. A strain gage can be bonded to the OD of the launch tube and monitored during the pressure cycle. The residual strain can then be read directly after the pressure is vented and interference axial forces calculated by the same methods as used in this experiment.

#### REFERENCES

1. Séférian, Daniel The Metallurgy of Welding. John Wiley & Sons, Inc., New York, 1962.
2. Cable, A. J. and Gillis, G. F. "Experience Obtained with Launch Tubes Repaired by Relining." Paper Presented at the 24th Meeting of the Aeroballistics Range Association, ARO, Inc., AEDC, Arnold Air Force Station, Tennessee, September 18-19, 1973.

3. Roark, Raymond J. Formulas for Stress and Strain.  
Third Edition, McGraw-Hill Book Company, Inc., New York, 1943.
4. Faupel, Joseph H. Engineering Design. John Wiley & Sons, Inc., New York, 1964.
5. Hoffman, Oscar and Sachs, George. Introduction to the Theory of Plasticity for Engineers. McGraw-Hill Book Company, Inc., New York, 1953.

Table 1. Measurements of Liner Movement for 013 Launch Tube

		Liner Protrusion	
Shot No.	Powder Weight, lb	Breech End, in.	Muzzle End, in.
2911	26.5	0.0015 to 0.0020	0.0085
2912	26.5	0.001	0.0105
2913	26.5	0.001	0.0105
	Next 2 Shots at 26.5		
2916	26.5	0.0035	
	Next Shot at 28		
2918	28	0.001 to 0.003	Remachined Flush

Table 2. Measurements of Liner Movement for 011 Launch Tube

Shot No.	Results
3027	Liner slipped downrange 0.023 in.
3028	Installed a 0.025-in.-thick aluminum spacer on uprange joint. Liner slipped downrange an additional 0.030 in. for a gap of 0.053 in. on this shot. This gap shifted to downrange joint during the piston removal process (the process applies a force in the uprange direction).
3029	Installed a 0.062-in. spacer on downrange joint. During this shot the gap increased an additional 0.098 in. for a total gap of 0.151 in. at the downrange joint. Liner moved uprange only 0.008 in. at uprange joint.
3030	Installed a 0.153-in. spacer on downrange joint. Liner moved an additional 0.055 in. for a total gap of 0.206 in. at the downrange joint. Liner moved uprange only 0.031 in. at uprange joint.
3031	Installed two spacers on downrange joint of 0.208-in. thickness. Installed a 0.035-in.-thick support shim at uprange joint.
3032	Launch tube removed from service after this shot.

Table 3. Dimensions of Components Tested

Test No.	Identification No.	Item	OD, in.	ID, in.	Length, in.	Diametral Clearance, in.
1	4A	Shell	7.002	3.0015	10.180	0.02
	14A	Liner	2.9815	2.4574	10.126	
2	4A	Shell	7.002	3.0015	10.180	0.0195
	14C	Liner	2.982	2.4576	10.129	
3	4B	Shell	6.998	3.0005	10.178	0.0185
	14B	Liner	2.982	2.4573	10.125	
4	54	Shell	10.983	3.0000	10.178	0.0181
	14H	Liner	2.9819	2.4572	10.033	
5	52	Shell	5.501	3.0025	10.1785	0.0181
	14D	Liner	2.9844	2.4572	10.128	
6	56	Shell	9.0065	3.0003	10.178	0.0173
	14G	Liner	2.983	2.4559	10.125	
7	4B	Shell	6.998	3.0005	10.178	0.0105
	50	Liner	2.990	2.4573	10.125	
8	4B	Shell	6.998	3.0005	10.178	0.024
	48	Liner	2.9765	2.4572	10.125	
9	4B	Shell	6.998	3.0005	10.178	0.0105
	51	Liner	2.990	2.4561	10.128	
10	4B	Shell	6.998	3.0005	10.178	0.0245
	49	Liner	2.976	2.4555	10.127	

- Notes: 1. The shell material was National Forge Co. NA 14 with  $\sigma_{ult} = 159,000$  psi and  $\sigma_y = 145,000$  psi.  
   2. The liner material was an extruded 1026 carbon steel with a quoted  $\sigma_{ult} = 85,000$  psi and  $\sigma_y = 75,000$  psi.

**Table 4. 7-in.-OD Shell with Medium-Fit Liner (0.020-in. Clearance)**  
**Tested for the Effect of Pressure Hold Time (Test No. 1)**

Cycle	Elapsed Time, $\Delta T$ , hr	Internal Pressure, $P_i$ , ksi	Circumferential Strain, $\epsilon_t$ , $\mu\text{in./in.}$ , avg	Longitudinal Strain, $\epsilon_\ell$ , $\mu\text{in./in.}$ , avg
1	0	21	55	0 0 0 18
	1.80	21	62	
	5.04	21	62	
	5.09	0	11	
At this point the test article was disassembled and component dimensions measured. Liner was still loose.				
2	0.30	51	475	-112
	0.65	49	471	-112
	1.65	49	464	-115
	2.90	49	461	-115
	5.01	49	458	-121
	5.06	0	- 15	- 11
	5.81	0	- 15	- 10
At this point the test article was disassembled and component dimensions measured. Liner was still loose.				
3	0.10	20	185	- 39
	0.22	50	492	-116
	0.45	75	765	--
	1.00	0	95*	48*

\*Test article was disassembled and liner was stuck. Residual strain reading inaccurate.

**Table 5. 7-in.-OD Shell with Medium-Fit Liner (0.020-in. Clearance)**  
**Tested for the Effect of Hold Time and Pressure Cycles**  
**(Test No. 2)**

Cycle	Elapsed Time, $\Delta T$ , hr	Internal Pressure, $P_i$ , ksi	Circumferential Strain, $\epsilon_t$ , $\mu\text{in./in.}$ , avg	Longitudinal Strain, $\epsilon_\ell$ , $\mu\text{in./in.}$ , avg
1	0	0	0	0
	0.62	18	32	- 6
	0.73	18	32	- 6
2	0.74	0	0	0
	0.81	18	30	- 6
	1.01	20	52	- 19
	1.09	20	50	- 20
3	1.12	0	- 10	- 10
	1.31	18	30	- 15
	1.32	20	40	- 17
	1.46	20	42	- 16
4	1.47	0	- 10	- 10
	1.54	20	52	- 21
	1.66	20	52	- 22
	1.69	29	180	- 46
	1.77	29	182	- 45
	1.79	20	95	- 29
	1.87	20	95	- 32
5	1.97	0	- 10	- 10
	2.01	20	89	- 28
	2.09	20	82	- 27
	2.14	29	185	- 49
	2.24	29	185	- 46
	2.26	20	90	- 33
	2.32	20	90	- 33
	2.34	0	- 11	- 10
6	2.41	0	- 10	- 10
	2.44	20	92	- 29
	2.49	20	90	- 28
	2.52	29	182	- 48
	2.60	29	184	- 49
	2.63	20	92	- 35
	2.71	20	90	- 35
	2.73	0	- 11	- 10
	2.81	0	- 10	- 10

Table 5. Continued.

Cycle	Elapsed Time, $\Delta T$ , hr	Internal Pressure, $P_i$ , ksi	Circumferential Strain, $\epsilon_t$ , $\mu\text{in./in.}$ , avg	Longitudinal Strain, $\epsilon_l$ , $\mu\text{in./in.}$ , avg
7	2.98	0	- 10	- 8
Equipment rezeroed prior to next cycle.				
	3.00	20	102	- 19
	3.10	20	100	- 19
	3.13	30	208	- 44
	3.21	30	206	- 45
	3.24	39	340	- 69
	3.34	39	342	- 68
	3.36	30	250	- 54
	3.44	30	248	- 55
	3.47	20	145	- 32
	3.55	20	145	- 29
8	3.57	0	0	0
	3.62	20	138	- 24
	3.69	20	138	- 24
	3.72	30	242	- 51
	3.77	39	345	- 75
	3.80	30	255	- 63
	3.83	20	150	- 37
9	3.85	0	0	0
	3.88	20	145	- 25
	3.92	30	249	- 50
	3.94	39	349	- 75
	3.99	30	260	- 64
	4.02	20	154	- 40
10	4.04	0	0	0
	4.09	20	142	- 25
	4.14	30	248	- 51
	4.17	40	351	- 75
	4.20	50	500	- 88
	4.28	50	500	- 99
	4.31	40	408	- 91
	4.39	40	401	- 89
	4.41	30	300	- 66
	4.43	20	199	- 37

Table 5. Continued

Cycle	Elapsed Time, $\Delta T$ , hr	Internal Pressure, $P_i$ , ksi	Circumferential Strain, $\epsilon_t$ , $\mu\text{in./in.}$ , avg	Longitudinal Strain, $\epsilon_\ell$ , $\mu\text{in./in.}$ , avg
11	4.45	0	0	0
	4.48	20	190	- 34
	4.51	30	295	- 59
	4.54	40	400	- 86
	4.57	50	510	-112
	4.65	50	510	-112
	4.68	40	412	-101
	4.71	30	308	- 76
	4.73	20	202	- 46
12	4.75	0	0	3
	4.80	20	200	- 35
	4.82	30	301	- 63
	4.85	40	409	- 89
	4.88	50	510	-114
	4.90	40	416	-103
	4.92	30	308	- 80
	4.95	20	209	- 50
	4.97	0	0	3
	5.32	0	0	11
	Broke down assembly and measured components. Liner was still loose.			
13	7.47	0	0	11
	7.49	20	201	- 40
	7.56	20	200	- 39
	7.59	30	301	- 65
	7.67	30	305	- 64
	7.70	40	410	- 91
	7.77	40	410	- 91
	7.80	50	515	-120
	7.87	34	372	- 93
	7.99	40	440	- 94
	8.02	50	541	-115
	8.05	60	648	-142

Table 5. Continued

Cycle	Elapsed Time, $\Delta T$ , hr	Internal Pressure, $P_i$ , ksi	Circumferential Strain, $\epsilon_t$ , $\mu\text{in./in.}$ , avg	Longitudinal Strain, $\epsilon_\ell$ , $\mu\text{in./in.}$ , avg
13 cont'd	8.33	58	631	-141
	8.36	60	650	-143
	8.43	60	649	-143
	8.45	50	558	-132
	8.50	50	550	-132
	8.52	39	444	-105
	8.55	28	330	- 78
	8.57	20	251	- 58
	8.59	0	25	13
14	8.86	0	28	11
Rezeroed strain gages.				
14	8.93	30	339	- 70
	9.01	30	338	- 70
	9.03	40	443	- 98
	9.06	50	546	-129
	9.14	59	638	-139
	9.21	59	647	-139
	9.23	50	553	-132
	9.31	50	548	-132
	9.33	40	448	-113
	9.41	40	447	-112
	9.44	30	346	- 87
	9.51	30	346	- 87
	9.53	20	239	- 57
	9.55	10	136	- 27
	9.57	5	79	- 8
	9.59	0	28	10
15	9.69	0	28	11
	9.76	20	239	- 40
	9.79	30	340	- 70
	9.86	40	448	- 99
	9.89	50	550	-122

Table 5. Continued

Cycle	Elapsed Time, $\Delta T$ , hr	Internal Pressure, $P_i$ , ksi	Circumferential Strain, $\epsilon_t$ , $\mu\text{in./in.}$ , avg	Longitudinal Strain, $\epsilon_\ell$ , $\mu\text{in./in.}$ , avg
15 cont'd	9.94	59	639	-144
	9.97	60	648	-143
	9.99	50	560	-139
	10.04	40	458	-117
	10.06	30	353	- 92
	10.08	20	242	- 58
	10.10	10	143	- 28
	10.12	5	89	- 9
16	10.15	0	28	10
	10.20	20	236	- 40
	10.23	30	340	- 70
	10.26	40	449	-102
	10.29	50	550	-125
	10.31	60	653	-145
	10.41	64	697	-153
	10.49	64	710	-154
	10.51	60	670	-153
	10.54	50	568	-140
	10.57	40	460	-119
	10.59	30	358	- 95
	10.61	18	233	- 53
	10.63	10	144	- 28
17	10.65	0	38	10
	10.70	20	248	- 40
	10.75	30	353	- 70
	10.77	40	460	- 99
	10.79	50	558	-122
	10.84	60	659	-145
	10.89	63	700	-153
	10.91	64	708	-154
	10.93	60	677	-154
	10.96	50	560	-140
	10.99	40	468	-119
	11.01	30	360	- 96
	11.04	20	258	- 60
	11.07	10	150	- 29

Table 5. Continued

Cycle	Elapsed Time, $\Delta T$ , hr	Internal Pressure, $P_i$ , ksi	Circumferential Strain, $\epsilon_t$ , $\mu\text{in./in.}$ , avg	Longitudinal Strain, $\epsilon_\ell$ , $\mu\text{in./in.}$ , avg
18	11.09	0	38	11
	11.14	20	248	- 40
	11.17	30	350	- 70
	11.20	40	459	- 99
	11.23	50	560	-123
	11.26	60	664	-145
	11.29	64	702	-153
	11.32	60	679	-153
	11.34	50	567	-139
	11.37	40	468	-119
	11.39	30	360	- 94
	11.41	20	259	- 63
	11.43	10	158	- 28
19	11.45	0	38	10
	11.50	20	249	- 39
	11.55	30	358	- 69
	11.77	40	468	- 98
	11.82	50	568	-121
	11.85	60	670	-142
	11.88	65	716	-150
	12.01	69	760	-155
	12.09	69	786	-159
	12.17	50	580	-137
	12.19	40	488	-118
	12.21	30	378	- 92
	12.23	20	279	- 59
	12.25	10	166	- 25
20	12.27	0	56	11
	12.32	20	263	- 39
	12.37	30	368	- 64
	12.40	40	479	- 94
	12.45	50	580	-119
	12.48	60	680	-140
	12.51	65	733	-149
	12.61	68	759	-154
	12.68	69	786	-159

Table 5. Continued

Cycle	Elapsed Time, $\Delta T$ , hr	Internal Pressure, $P_i$ , ksi	Circumferential Strain, $\epsilon_t$ , $\mu\text{in./in.}$ , avg	Longitudinal Strain, $\epsilon_\ell$ , $\mu\text{in./in.}$ , avg
20 cont'd	12.70	65	758	-159
	12.73	60	708	-155
	12.76	50	588	-136
	12.79	40	488	-117
	12.81	30	388	- 94
	12.83	20	282	- 60
	12.85	10	169	- 26
	12.87	0	58	10
	12.95	0	58	11
21	13.85	0	58	11
	13.95	20	260	- 40
	14.00	30	368	- 69
	14.03	40	478	- 98
	14.08	50	579	-122
	14.10	60	687	-143
	14.13	65	736	-149
	14.25	65	738	-151
	14.30	68	768	-155
	14.35	69	786	-157
	14.42	57	660	-148
	14.45	50	593	-136
	14.47	40	489	-116
	14.50	30	389	- 96
	14.52	20	284	- 59
	14.54	10	174	- 22
22	14.56	0	60	10
	14.61	20	270	- 38
	14.66	30	378	- 65
	14.69	40	488	- 96
	14.72	50	589	-121
	14.75	60	689	-143
	14.77	65	729	-146
	14.80	67	768	-159
	14.85	70	778	-164
	14.93	70	807	-171
	14.96	74	830	-174
	14.99	50	607	-148
	15.01	30	394	- 96

Table 5. Concluded

Cycle	Elapsed Time, $\Delta T$ , hr	Internal Pressure, $P_i$ , ksi	Circumferential Strain, $\epsilon_t$ , $\mu\text{in./in.}$ , avg	Longitudinal Strain, $\epsilon_\ell$ , $\mu\text{in./in.}$ , avg
23	15.04	0	68	9
	15.09	30	379	- 67
	15.16	50	596	-120
	15.21	68	778	-164
	15.29	73	829	-173
	15.31	77	859	---
	15.34	50	604	-146
	15.41	74	829	-170
	15.49	75	860	-177
	15.51	67	800	-176
	15.53	58	700	-165
	15.58	50	610	-148
	15.60	30	400	- 98
24	15.62	0	74	7
	15.77	30	386	- 69
	15.82	50	600	-129
	15.87	67	783	-164
	15.94	74	843	-174
	15.99	74	859	-179
	16.01	50	616	-150
	16.03	73	848	-177
	16.11	73	849	-175
	16.19	73	850	-174
	16.27	73	849	-174
	16.35	73	848	-175
	16.42	75	868	-179
	16.52	74	868	-175
	16.60	74	868	-177
	16.68	74	867	-180
	16.70	50	617	-150
	16.72	30	416	-104
	16.75	0	77	5
	16.85	0	78	6
	16.90	0	77	5

Readings taken to monitor gage drift.

**Table 6. 7-in.-OD Shell with Medium-Fit Liner (0.0185-in. Clearance)  
Tested for the Effect of Liner Clearance (Test No. 3)**

Cycle	Elapsed Time, $\Delta T$ , hr	Internal Pressure, $P_i$ , ksi	Circumferential Strain, $\epsilon_t$ , $\mu\text{in./in.}$ , avg	Longitudinal Strain, $\epsilon_\ell$ , $\mu\text{in./in.}$ , avg
1	0	0	0	0
	0.03	20	55	- 9
	0.27	30	---	---
	Leak developed in the supply line.			
	0.48	20	90	- 19
	0.55	30	194	- 41
	0.63	50	---	---
	Leak developed in intensifier.			
	0.68	28	210	- 50
	0.70	20	141	- 30
2	0.77	0	7	6
	1.05	0	2	0
	1.08	0	0	0
	Repaired leaky intensifier and rezeroed strain gages.			
	1.16	20	128	- 30
	1.23	40	336	- 88
	1.58	60	666	-143
	1.66	70	773	-165
	Seals in test rig leaked slightly.			
	1.76	59	675	-151
	1.95	68	759	-160
	2.06	74	834	-170
	2.11	71	802	- 70
	2.16	60	700	-151
	2.20	40	490	- 98
	2.25	19	279	- 46

Table 6. Concluded

Cycle	Elapsed Time, $\Delta T$ , hr	Internal Pressure, $P_i$ , ksi	Circumferential Strain, $\epsilon_t$ , $\mu\text{in./in.}$ , avg	Longitudinal Strain, $\epsilon_\ell$ , $\mu\text{in./in.}$ , avg
3	2.30	0	80	- 9
	2.36	20	269	- 35
	2.41	40	466	- 80
	2.50	60	680	-135
	2.55	70	760	---
	Seals leaked slightly.			
	2.60	50	685	-130
	2.66	52	701	-141
	2.68	70	782	---
	Seals leaked slightly.			
4	2.70	60	693	-150
	2.73	40	485	-100
	2.75	14	221	- 27
	2.78	0	75	11
	3.45	0	72	8
	Disassembled test article and replaced seals.			
	6.66	0	75	25
	7.00	20	270	- 19
	7.05	40	471	- 66
	7.08	60	682	-128
	7.58	61	700	-130
	New seals leaked.			
	7.60	40	489	- 96
	7.63	20	281	- 33
	7.65	0	75	30
	8.03	0	75	27
Readings taken to monitor gage drift.				

**Table 7. 7-in.-OD Shell with Tight-Fit Liner (0.0105-in. Clearance)  
Tested for the Effect of Liner Clearance (Test No. 7)**

Cycle	Elapsed Time, $\Delta T$ , hr	Internal Pressure, $P_i$ , ksi	Circumferential Strain, $\epsilon_t$ , $\mu\text{in./in.}$ , avg	Longitudinal Strain, $\epsilon_\ell$ , $\mu\text{in./in.}$ , avg
1	0	0	0	0
	0.17	20	49	- 10
	0.25	40	335	- 69
	0.28	60	624	-119
	0.32	70	766	-139
	0.33	75	835	-150
	0.42	70	795	-150
	0.45	60	692	-135
	0.48	40	486	- 84
	0.50	0	72	20
2	0.55	0	72	20
	0.58	20	270	20
	0.67	40	463	- 70
	0.70	60	669	-120
	0.75	70	776	-141
	0.78	75	838	-150
	0.83	70	796	-150
	0.85	60	693	-135
	0.88	40	487	- 89
	0.92	20	289	- 29
	0.95	0	78	20
	1.15	0	85	35
Reading taken to monitor gage drift.				

**Table 8. 7-in.-OD Shell with Tight-Fit Liner (0.0105-in. Clearance)  
Tested for the Effect of Liner Clearance (Test No. 9)**

Cycle	Elapsed Time, $\Delta T$ , hr	Internal Pressure, $P_i$ , ksi	Circumferential Strain, $\epsilon_t$ , $\mu\text{in./in.}$ , avg	Longitudinal Strain, $\epsilon_\ell$ , $\mu\text{in./in.}$ , avg
1	0	0	0	0
	0.47	20	51	- 10
	0.49	40	322	- 79
	0.57	60	600	-131
	0.65	70	730	-159
	0.70	75	790	-169
	0.75	70	740	-163
	0.77	60	645	-152
	0.79	40	465	-105
	0.81	20	267	- 38
2	0.84	0	61	11
	0.91	20	248	- 28
	0.94	40	429	- 79
	1.01	60	627	-130
	1.04	70	730	-158
	1.07	75	786	-164
	1.09	70	737	-161
	1.12	60	646	-151
	1.14	40	456	-115
	1.19	20	268	- 54
	1.22	0	70	8
	1.27	20	250	- 29
3	1.29	40	434	- 80
	1.36	60	634	-130
	1.38	70	734	-155
	1.43	75	788	-165
	1.53	70	736	-162
	1.55	60	644	-150
	1.57	40	452	-122
	1.59	20	268	- 50
	1.61	0	69	10
	1.71	0	73	21
Reading taken to monitor gage drift.				

**Table 9. 7-in.-OD Shell with Loose-Fit Liner (0.024-in. Clearance)  
Tested for the Effect of Liner Clearance (Test No. 8)**

Cycle	Elapsed Time, $\Delta t$ , hr	Internal Pressure, $P_1$ , ksi	Circumferential Strain, $\epsilon_t$ , $\mu\text{in./in.}$ , avg	Longitudinal Strain, $\epsilon_\ell$ , $\mu\text{in./in.}$ , avg
1	0	0	0	0
Seals in this test were also used for a previous test.				
	0.30	20	45	-18
	0.35	40	340	-80
	0.43	60	626	-119
	0.50	70	761	-150
	0.55	75	830	---
Seals leaked slightly.				
	0.58	64	725	-140
	0.62	70	781	-142
	0.70	75	835	-156
Seals held for approximately two minutes then leaked slightly.				
	0.75	60	686	-127
	0.78	40	481	-94
	0.80	20	276	-35
2	0.82	0	51	10
	0.87	20	256	-37
	0.90	40	446	-87
	0.98	60	663	-121
Seals leaked slightly.				
	1.08	58	662	-120
	1.13	60	683	-115
	1.17	65	735	-127
	1.20	70	770	-155
Seals leaked slightly.				
	1.25	65	726	-146
	1.35	70	773	-151
	1.42	75	827	-160
Seals leaked slightly.				
	1.47	61	688	-137
	1.50	65	735	-140
	1.58	70	786	-151
	1.83	75	835	-160
Seals leaked slightly.				
	1.87	60	686	-131
	1.90	40	476	-90
	1.92	20	277	-38
	1.93	0	56	12
	2.08	0	58	14
Reading taken to monitor gage drift.				

**Table 10. 7-in.-OD Shell with Loose-Fit Liner (0.0245-in. Clearance)  
Tested for the Effect of Liner Clearance (Test No. 10)**

Cycle	Elapsed Time, $\Delta T$ , hr	Internal Pressure, $P_i$ , ksi	Circumferential Strain, $\epsilon_t$ , $\mu\text{in./in.}$ , avg	Longitudinal Strain, $\epsilon_\ell$ , $\mu\text{in./in.}$ , avg
1	0	0	0	0
	0.34	20	50	- 10
	0.39	40	314	- 69
	0.44	60	590	-118
	0.54	70	720	-141
	0.57	75	781	-151
	0.64	70	737	-151
	0.67	60	634	-137
	0.70	40	444	- 92
	0.72	20	245	- 37
2	0.74	0	45	9
	0.77	20	234	- 29
	0.80	40	417	- 71
	0.87	60	623	-130
	0.89	70	725	-151
	0.92	75	782	-162
	0.99	70	738	-159
	1.01	60	635	-141
	1.04	40	436	- 99
	1.06	20	245	- 39
	1.08	0	47	7
	1.13	20	237	- 29
3	1.18	40	425	- 80
	1.21	60	624	-129
	1.24	70	724	-150
	1.27	75	777	-160
	1.32	70	738	-156
	1.34	57	611	-135
	1.36	40	438	- 99
	1.39	18	226	- 40
	1.42	0	50	9
	1.47	0	55	20
Reading taken to monitor gage drift.				

**Table 11. 5.5-in.-OD Shell with Medium-Fit Liner (0.0181-in. Clearance)  
Tested for the Effect of Launch Tube OD (Test No. 5)**

Cycle	Elapsed Time, $\Delta T$ , hr	Internal Pressure, $P_i$ , ksi	Circumferential Strain, $\epsilon_t$ , $\mu\text{in./in.}$ , avg	Longitudinal Strain, $\epsilon_\ell$ , $\mu\text{in./in.}$ , avg
1	0	0	0	0
	0.03	20	56	- 40
	0.20	40	553	-161
	0.27	50	806	-214
	0.45	55	950	-240
	0.52	60	1066	-275
	0.62	50	916	-235
	0.63	40	732	-196
	0.67	20	405	- 83
2	0.70	0	62	10
	0.77	20	378	- 81
	0.80	40	707	-183
	0.85	50	864	-226
	0.92	60	1066	-279
	1.00	50	895	-237
	1.02	40	734	-187
	1.05	20	413	- 98
	1.08	0	69	8
3	1.13	20	387	- 79
	1.17	40	715	-179
	1.25	60	1076	-277
	1.42	40	744	-185
	1.45	20	420	- 95
	1.50	0	79	13
	1.58	0	81	30
Last reading taken to monitor gage drift.				

Table 12. 9-in.-OD Shell with Medium-Fit Liner (0.0173-in. Clearance)  
Tested for the Effect of Launch Tube OD (Test No. 6)

Cycle	Elapsed Time, $\Delta T$ , hr	Internal Pressure, $P_i$ , ksi	Circumferential Strain, $\epsilon_t$ , $\mu\text{in./in.}$ , avg	Longitudinal Strain, $\epsilon_\ell$ , $\mu\text{in./in.}$ , avg
1	0	0	0	0
	0.02	15	0	- 1
	0.03	16	0	- 1
	0.05	17	0	- 1
	0.07	18	5	0
	0.12	20	20	- 1
	0.15	40	180	- 26
	0.17	60	340	- 56
	0.27	70	417	- 72
	Seals leaked slightly.			
	0.33	53	336	- 81
	0.35	70	440	---
	Seals leaked slightly.			
	0.47	70	435	- 78
	0.52	80	496	- 90
	Seals leaked slightly.			
	0.60	53	347	- 80
	0.68	53	350	- 77
2	0.73	70	445	- 76
	0.85	75	475	- 81
	0.92	80	505	- 86
	1.00	85	536	- 95
	1.08	80	515	- 100
	1.13	60	398	- 94
	1.17	40	285	- 78
	1.18	20	171	- 52
	1.20	0	51	- 26
	1.30	20	156	- 24
	1.35	40	266	- 46
	1.40	60	385	- 74
	1.42	70	445	- 86
	1.52	73	461	---
O-Ring seal blew out of test article.				
	1.60	0	55	- 29
	1.93	0	56	- 27
Reading taken to monitor gage drift.				

**Table 13. 11-in.-OD Shell with Medium-Fit Liner (0.0181-in. Clearance)  
Tested for the Effect of Launch Tube OD (Test No. 4)**

Cycle	Elapsed Time, $\Delta T$ , hr	Internal Pressure, $P_i$ , ksi	Circumferential Strain, $\epsilon_t$ , $\mu\text{in./in.}$ , avg	Longitudinal Strain, $\epsilon_\ell$ , $\mu\text{in./in.}$ , avg
1	0	0	0	0
	0.38	20	14	0
	0.45	40	110	- 8
	0.48	60	208	- 28
	0.52	70	256	- 30
	Developed leak in intensifier, had to abort for repairs.			
	0.63	60	222	- 39
	0.65	40	152	- 30
	0.67	20	79	- 20
	0.70	0	7	0
2	0.77	20	77	- 9
	0.82	40	148	- 20
	0.85	60	220	- 29
	0.88	70	256	- 30
	Seals leaked slightly.			
	0.93	43	173	- 35
	0.98	70	267	- 31
	Seals leaked slightly.			
	1.03	40	160	- 36
	1.05	60	231	- 30
3	1.15	70	266	- 31
	Seals leaked slightly.			
	1.20	39	158	- 35
	1.22	20	88	- 20
	1.23	0	15	- 1
	2.65	20	84	- 9
	2.68	40	155	- 20
	2.77	60	227	- 30

Table 13. Continued

Cycle	Elapsed Time, $\Delta T$ , hr	Internal Pressure, $P_i$ , ksi	Circumferential Strain, $\epsilon_t$ , $\mu\text{in./in.}$ , avg	Longitudinal Strain, $\epsilon_l$ , $\mu\text{in./in.}$ , avg
3 cont'd	2.85	70	266	- 30
	2.95	75	283	- 32
	Seals leaked slightly.			
	3.05	43	171	- 37
	3.12	43	168	- 38
	3.32	70	264	- 30
	Seals leaked slightly.			
	3.43	42	166	- 32
	3.48	60	229	- 30
	3.67	70	263	- 35
	3.75	75	282	- 36
	3.80	80	---	---
	Seals leaked slightly.			
	3.88	45	176	- 41
	3.95	40	160	- 40
	3.98	20	88	- 21
	4.02	0	16	- 1
	4.58	0	19	0
	Disassembled, installed new seal on nut end. Number 2 circumferential gage damaged during disassembly.			
4	0	0	21	0
	0.95	20	91	- 4
	0.98	40	160	- 19
	1.03	60	235	- 31
	Seals leaked slightly.			
	1.10	70	272	- 39
	1.12	75	291	- 41
	Seals leaked slightly.			

Table 13. Concluded

Cycle	Elapsed Time, $\Delta T$ , hr	Internal Pressure, $P_i$ , ksi	Circumferential Strain, $\epsilon_t$ , $\mu\text{in./in.}$ , avg	Longitudinal Strain, $\epsilon_\ell$ , $\mu\text{in./in.}$ , avg
4 cont'd	1.22	75	294	- 41
	1.28	80	310	- 44
	1.30	85	332	- 46
	1.33	90	355	- 50
	1.37	90	361	- 53
	1.38	80	325	- 54
	1.40	60	250	- 50
	1.42	40	180	- 46
	1.43	20	105	- 33
5	1.45	0	28	- 8
	1.55	20	98	- 14
	1.58	40	162	- 25
	1.62	60	240	- 35
	1.68	80	320	---
Seals leaked slightly.				
	1.73	54	225	- 49
	1.75	60	247	- 46
	1.83	70	281	- 44
	1.95	75	300	- 45
Seals leaked slightly.				
	2.03	54	225	- 46
	2.12	70	282	- 44
	2.18	75	300	- 44
	2.23	80	320	- 45
	2.37	90	360	- 46
	2.50	80	330	- 53
	2.53	60	252	- 55
	2.55	40	182	- 46
	2.57	20	105	- 26
	2.50	0	28	- 6
	2.83	0	30	- 1
	Reading taken to monitor gage drift.			

Table 14. Liner and Shell Dimensions after Completion of Axial-Force Test

Test No.	Identification No.	Item	OD, in.	ID, in.	Length, in.	$\delta$ , in.	$P_{c\delta}^1$ , psi	$P_{c\epsilon}^2$ , psi
5	52 14D	Shell Liner	5.501 3.0041	3.002 2.4803	10.179 10.109	0.0011	2,941	2,869
8	4B 48	Shell Liner	6.9983 3.0039	3.0007 2.4898	10.178 10.10	0.0016	4,654	3,800
10	4B 49	Shell Liner	6.9983 3.004	3.0007 2.4878	10.178 10.117	0.0017	4,815	3,667

- Notes: 1.  $P_{c\delta}$  - Interference pressure calculated for the measured interference,  $\delta$ .  
 2.  $P_{c\epsilon}$  - Interference pressure calculated for the measured residual strain,  $\epsilon$ .

Table 15. Typical Liner Dimension Changes during Testing

Cycle	Identification No.	OD, in.	ID, in.	Length, in., avg	Liner Thickness, in.
Original Dimensions	14A	2.9815	2.4574	10.126	0.2621
1	14A	2.995	2.4723	10.107	0.2614
2	14A	3.0015	2.480	10.102	0.2608
3	14A	3.0015	2.481	10.1035	0.2603

## APPENDIX A BASIC STRESS EQUATIONS

### A-1 CLOSED-END VESSEL

The well known Lamé equations for the elastic stress distribution and deflection of a thick walled, closed pressure vessel subjected to internal pressure are:

$$\sigma_r = \frac{a^2 p_i}{b^2 - a^2} \left( 1 - \frac{b^2}{r^2} \right) \quad (A-1)$$

$$\sigma_\ell = \frac{a^2 p_i}{b^2 - a^2} \quad (A-2)$$

$$\sigma_t = \frac{a^2 p_i}{b^2 - a^2} \left( 1 + \frac{b^2}{r^2} \right) \quad (A-3)$$

and

$$u = \frac{p_i a^2}{E(b^2 - a^2)} \left[ (1 - 2\nu)r + (1 + \nu) b^2/r \right] \quad (A-4)$$

where

$\sigma_r$  = radial component of stress = psi,

$\sigma_\ell$  = axial component of stress = psi,

$\sigma_t$  = circumferential component of stress = psi,

$u$  = radial deflection = in.,

$p_i$  = applied pressure = psi,

$\nu$  = Poisson's ratio,

$a$  = inside radius of the vessel = in.,

$b$  = outside radius of the vessel = in.,

and

$E$  = modulus of elasticity = lb/in.<sup>2</sup>

Most pressure vessels are designed on the basis of these equations so that the stress never exceeds the yield strength of the material. When vessels are to be designed for the maximum limits of operation, a theory of failure has to be used in conjunction with these equations to predict failure conditions. The most widely accepted one for pressure vessels fabricated from ductile materials is the distortion energy theory (von Mises-Hencky criterion) of failure. By this theory

$$2\sigma_y^2 = (\sigma_r - \sigma_\ell)^2 + (\sigma_f - \sigma_t)^2 + (\sigma_r - \sigma_t)^2 \quad (A-5)$$

where

$\sigma_y$  = the yield strength of the material = psi.

In words, Eq. (A-5) states that when the stress state is such that the right side of the equation equals two times the square of the material yield strength, the vessel is in a state of incipient yielding. If the right side is less than the left, then no yielding should occur. If the right side is larger, yielding should occur at some lower pressure level. Thus, Eqs. (A-1) through (A-3) and Eq. (A-5) can be used to determine the pressure just sufficient to cause bore yielding. Evaluation of Eqs. (A-1) through (A-3) at  $r = a$  and substitution of the results into Eq. (A-5) yields

$$P_y = \frac{\sigma_y}{\sqrt{3}} \left( \frac{K^2 - 1}{K^2} \right) \quad (A-6)$$

where

$P_y$  = pressure just sufficient to cause bore yielding = psi

and

$K$  = ratio of  $b$  to  $a$ .

If the pressure exceeds  $P_y$ , the vessel will have an inner plastic zone surrounded by an elastic outer one. The stresses in the inner plastic zone are defined by Ref. 5, i.e.,

$$\sigma_r = \frac{\sigma_y}{\sqrt{3}} \left( 2 \ln \frac{r}{\rho} - 1 + \frac{\rho^2}{b^2} \right) \quad (A-7)$$

$$\sigma_\ell = \frac{\sigma_y}{\sqrt{3}} \left( 2 \ln \frac{r}{\rho} + 1 + \frac{\rho^2}{b^2} \right) \quad (A-8)$$

and

$$\sigma_t = \frac{\sigma_y}{\sqrt{3}} \left( 2 \ln \frac{r}{\rho} + 1 + \frac{\rho^2}{b^2} \right) \quad (A-9)$$

The stresses in the outer elastic zone are

$$\sigma_r = \frac{\sigma_y}{\sqrt{3}} \left( \frac{\rho^2}{b^2} - \frac{\rho^2}{r^2} \right) \quad (A-10)$$

$$\sigma_\ell = \frac{\sigma_y}{\sqrt{3}} \frac{\rho^2}{b^2} \quad (A-11)$$

and

$$\sigma_t = \frac{\sigma_y}{\sqrt{3}} \left( \frac{\rho^2}{b^2} + \frac{\rho^2}{r^2} \right) \quad (A-12)$$

where

$\rho$  = radius of the plastic front = in.

A relation between the applied pressure and the radius of the plastic front,  $\rho$ , can be obtained by recognizing that Eq. (A-7) must still equal minus  $P$  at the vessel inner radius  $r = a$ . Thus,

$$\frac{P}{\rho} = \frac{\sigma_y}{\sqrt{3}} \left( 2 \ln \frac{\rho}{a} + 1 - \frac{\rho^2}{b^2} \right) \quad (A-13)$$

$\frac{P}{\rho}$  = pressure to cause yielding to a radius  
 $\rho$  = psi.

Full plasticity occurs when the plastic front has progressed to the outer radius of the vessel; hence, from Eq. (A-13), with  $\rho = b$ ,

$$P_f = \frac{2 \sigma_y}{\sqrt{3}} \ln K \quad (A-14)$$

where

$P_f$  = full-wall yield pressure.

By the general theory of plasticity, yielding will progress through the wall at constant stress, i.e., Eqs. (A-7) through (A-9) will satisfy Eq. (A-5). For vessels whose ultimate is greater than its yield strength, bursting should occur after the wall has completely yielded. Faupel (Ref. 4) postulates that burst of the vessel will be governed by the expression

$$P_b = \frac{2 \sigma_y \ln K}{\sqrt{3}} \left( 2 - \frac{\sigma_y}{\sigma_u} \right) \quad (A-15)$$

where

$P_b$  = burst pressure = psi

and

$\sigma_u$  = material ultimate strength = psi.

The equation represents an attempt to average the effects of an ultimate higher than the yield. Obviously, if  $\sigma_y = \sigma_u$  then  $P_f = P_b$ ; however, if  $\sigma_u > \sigma_y$  then  $P_b > P_f$ .

The above equations are applicable for the launch tube during the autofrettage process, i.e., the bore yield can be calculated by Eq. (A-6), full-wall yield by Eq. (A-14), and burst by Eq. (A-15).

## A-2 OPEN-END VESSEL WITH A PRESSURE END LOAD

The liner for the launch tube autofrettage setup can be analyzed as an open-ended vessel with the pressure applied to the bore and to the ends of the open vessel. Equations (A-1) and (A-3) are still applicable; however, Eq. (A-2) becomes

$$\sigma_\ell = -P_i \quad (A-16)$$

Substitution of Eqs. (A-1), (A-3), and (A-16) evaluated at  $r = a$ , into Eq. (A-5) yields

$$p_y = \frac{(K^2 - 1)}{2K^2} \sigma_y \quad (A-17)$$

Note that bore yield pressures calculated from Eq. (A-6) will be about 15.5 percent higher than those calculated from Eq. (A-17) for the dimensions of interest in this report. Thus, more pressure is required to yield a closed-end vessel than an open one which has a compressive axial stress equal to the applied pressure.

Once the applied pressure exceeds the value calculated from Eq. (A-17), an inner zone of the vessel becomes plastic. Others have shown that one may assume

$$\sigma_\ell = \frac{1}{2} (\sigma_t + \sigma_r) \quad (A-18)$$

an exact relationship for the elastic zone - see Eqs. (A-1), (A-2), and (A-3) in this region for long, closed vessels subject to either external or internal pressure. This is equivalent to assuming plane strain ( $\epsilon_\ell = 0$ ) exists in the plastic zone. Obviously this is not exactly true since there is a strain in the elastic zone caused by the pressure force in the axial direction and the transition between the elastic and plastic zones should be continuous. The justification for the assumption is that the plane strain case is easier to derive, is approximately correct for long vessels, and is exactly correct for the elastic region.

If the assumption is made that Eq. (A-18) also holds for the open-end vessel with a pressure end load and Eq. (A-18) is substituted into Eq. (A-5), the results are

$$\sigma_t - \sigma_r = \frac{2\sigma_y}{\sqrt{3}} \quad (A-19)$$

for the plastic zone.

The governing equilibrium equation, which is valid throughout the cylinder, is

$$\frac{d\sigma_r}{dr} = \frac{1}{r} (\sigma_t - \sigma_r). \quad (A-20)$$

Substitution of Eq. (A-19) into Eq. (A-20) and integration of the results yields

$$\sigma_r = \frac{2\sigma_y}{\sqrt{3}} \ln r + c_1 \quad (A-21)$$

where  $c_1$  is a constant of integration.

Equation (A-21) applies to the inner plastic zone; however, it is also valid at the elastic-plastic interface. At this interface, denoted by radius  $r = \rho$ , the radial stress is just sufficient to cause incipient yielding of the outer elastic zone. Thus, from Eq. (A-17)

$$\sigma_r = -p_y = -\frac{\left(\frac{b^2}{2} - 1\right)}{2 \frac{b^2}{2} \rho} \sigma_y \quad (A-22)$$

The constant  $c_1$  in Eq. (A-21) can be evaluated by equating Eqs. (A-21) and (A-22) at  $r = \rho$ . Substitution of this result in Eq. (A-21) yields

$$\sigma_r = \sigma_y \left( \frac{2}{\sqrt{3}} \ln \frac{r}{\rho} - \frac{b^2 - \rho^2}{2b^2} \right) \quad (A-23)$$

The hoop and axial stresses in the plastic zone can be obtained by substitution of Eq. (A-23) into Eqs. (A-18) and (A-19), i.e.,

$$\sigma_t = \sigma_y \left[ \frac{2}{\sqrt{3}} \left( 1 + \ln \frac{r}{\rho} \right) - \frac{b^2 - \rho^2}{2b^2} \right] \quad (A-24)$$

$$\sigma_\ell = \sigma_y \left[ \frac{2}{\sqrt{3}} \left( \frac{1}{2} + \ln \frac{r}{\rho} \right) - \frac{b^2 - \rho^2}{2b^2} \right] \quad (A-25)$$

The pressure required to fully yield the wall can be obtained from Eq. (A-23) by the substitution  $\sigma_r = -p_i$ ,  $r = a$ , and  $\rho = b$ . Thus,

$$P_f = \frac{2}{\sqrt{3}} \sigma_y \ln K \quad (A-26)$$

Note that Eqs. (A-26) and (A-14) are identical. This means, obviously, that the same internal pressure will cause full-wall yielding for both cases.

Since the bore yield pressure is lower for the open-end vessel with an applied compressive end load, one would reasonably expect a lower full-wall yield pressure. The inaccuracy results directly from the assumption that Eq. (A-18) is valid in the plastic region. By manipulation of Eqs. (A-16), (A-1), and (A-3) it can be shown that

$$\sigma_\ell = \frac{\sigma_r + \sigma_t}{2} - \frac{\sigma_t - \sigma_r}{2} \left( \frac{r^2}{a^2} \right) \quad (A-27)$$

in the elastic vessel. Perhaps a more reasonable assumption for the plastic zone would be that Eq. (A-27) rather than Eq. (A-18) is applicable. The derivation that follows is based on this premise.

Substitution of Eq. (A-27) into the yield condition of Eq. (A-5) yields

$$\sigma_t - \sigma_r = \frac{2a^2 \sigma_y}{\sqrt{3a^4 + r^4}} \quad (A-28)$$

With this result, the equilibrium equation, Eq. (A-20), can be written

$$\sigma_r = 2 \sigma_y a^2 \int \frac{dr}{r \sqrt{3a^4 + r^4}} \quad (A-29)$$

Let  $x = r^2$ , to change the above to a standard form suitable for integration, then Eq. (A-29) becomes

$$\sigma_r = \sigma_y a^2 \int \frac{dx}{x \sqrt{3a^4 + x^2}} \quad (A-30)$$

and

$$\sigma_r = -\frac{\sigma_y}{\sqrt{3}} \operatorname{csch}^{-1} \frac{r^2}{a^2 \sqrt{3}} + c_2 \quad (\text{A-31})$$

The constant of integration can be evaluated from the boundary condition

$$\sigma_r = -p_y = \frac{b^2 - \rho^2}{2b^2} \sigma_y \text{ at } r = \rho \quad (\text{A-32})$$

Thus, Eq. (A-31) becomes

$$\sigma_r = \frac{\sigma_y}{2} \left[ \frac{2}{\sqrt{3}} \left( \operatorname{csch}^{-1} \frac{\rho^2}{a^2 \sqrt{3}} - \operatorname{csch}^{-1} \frac{r^2}{a^2 \sqrt{3}} \right) - 1 + \frac{\rho^2}{b^2} \right] \quad (\text{A-33})$$

Substitution of Eq. (A-33) into Eq. (A-28) yields

$$\begin{aligned} \sigma_t &= \frac{\sigma_y}{2} \left[ \frac{2}{\sqrt{3}} \left( \operatorname{csch}^{-1} \frac{\rho^2}{a^2 \sqrt{3}} - \operatorname{csch}^{-1} \frac{r^2}{a^2 \sqrt{3}} \right) \right. \\ &\quad \left. - 1 + \frac{\rho^2}{b^2} + \frac{4a^2}{\sqrt{3a^4 + r^4}} \right] \end{aligned} \quad (\text{A-34})$$

The relationship between the applied internal pressure and the radius of the plastic front can be obtained from Eq. (A-33) by applying the boundary conditions

$$\sigma_r = -p_i \text{ at } r = a$$

Thus,

$$p_\rho = \frac{\sigma_y}{2} \left[ \frac{2}{\sqrt{3}} \left( \operatorname{csch}^{-1} \frac{1}{\sqrt{3}} - \operatorname{csch}^{-1} \frac{\rho^2}{a^2 \sqrt{3}} \right) + 1 - \frac{\rho^2}{b^2} \right] \quad (\text{A-35})$$

Full plasticity is reached when the radius of the plastic front extends to  $\rho = b$ , i.e.,

$$p_f = \frac{\sigma_y}{\sqrt{3}} \left( \operatorname{csch}^{-1} \frac{1}{\sqrt{3}} - \operatorname{csch}^{-1} \frac{b^2}{\sqrt{3}} \right) \quad (\text{A-36})$$

For comparison purposes, assume a pressure vessel with an OD = 3 in. and an ID = 2.5 in. For Case 1, consider a closed vessel with an internal pressure. Equations (A-6) and (A-14) apply and yield

$$P_{y1} = 0.176 \sigma_y \quad (A-37)$$

and

$$P_{f1} = 0.211 \sigma_y \quad (A-38)$$

For Case 2, consider an open vessel with the pressure acting on the bore and the ends. Equations (A-17) and (A-36) apply and yield

$$P_{y2} = 0.153 \sigma_y \quad (A-39)$$

and

$$P_{f2} = 0.173 \sigma_y \quad (A-40)$$

Note that the ratios between corresponding pressures have the following values

$$\frac{P_{y1}}{P_{y2}} = 1.15 \quad (A-41)$$

and

$$\frac{P_{f1}}{P_{f2}} = 1.22 \quad (A-42)$$

If the usual plane strain assumption had been made for Case 2, Eqs. (A-17) and (A-26) would apply. Thus, the ratio of Eq. (A-41) would have the same value and the ratio of Eq. (A-42) would be equal to one. That is, the closed-end vessel would require 15 percent more pressure for bore yield than the open-end one; however, they would both reach full-wall yield at the same pressure. This result would be counter to normal logic. The trend shown in Eqs. (A-41) and (A-42) are more logical and tend to verify the assumption made in Eq. (A-27). Hence, it will be assumed that the liner for the launch tubes will be governed by Eqs. (A-17) and (A-36) during the autofrettage procedure.

**A-3 OPEN-END VESSEL WITHOUT END LOAD**

The autofrettage test article described in this report involves a liner which can be considered an open-end pressure vessel without any axial load. For these conditions, Eqs. (A-1) and (A-3) are still applicable and Eq. (A-2) becomes

$$\sigma_\ell = 0 \quad (\text{A-43})$$

Substitution of Eqs. (A-1), (A-3), and (A-43) into Eq. (A-5) evaluated at  $r = a$  yields

$$p_y = \frac{(K^2 - 1) \sigma_y}{\sqrt{1 + 3K^4}} \quad (\text{A-44})$$

for the bore yield pressure.

Hoffman and Sachs (Ref. 5) show that

$$\frac{d\sigma_r}{dr} - \frac{\sqrt{4\sigma_y^2 - 3\sigma_r^2} - \sigma_r}{2r} = 0 \quad (\text{A-45})$$

may be obtained by solving Eq. (A-5) for  $\sigma_t$  and substituting the results into Eq. (A-20). The quoted reference also shows that the solution of this equation is

$$\ln r = \frac{\sqrt{3}}{2} \sin^{-1} \left( \frac{\sqrt{3}}{2} \frac{\sigma_r}{\sigma_y} \right) - \frac{1}{2} \ln \left( \sqrt{1 - \frac{3\sigma_r^2}{4\sigma_y^2}} - \frac{\sigma_r}{2\sigma_y} \right) + c_3 \quad (\text{A-46})$$

where

$$c_3 = \ln b$$

Equation (A-46) governs in the plastic zone for the vessel; hence, if the vessel is in a state of full plasticity

$$\sigma_r = -p_f \text{ at } r = a$$

and

$$-\ln K = \frac{\sqrt{3}}{2} \sin^{-1} \left( -\frac{\sqrt{3}}{2} \frac{p_f}{\sigma_y} \right) - \frac{1}{2} \ln \left( \sqrt{1 - \frac{3p_f^2}{4\sigma_y^2}} + \frac{p_f}{2\sigma_y} \right) \quad (A-47)$$

Equation (A-47) holds for the liner in the autofrettage test rig up to the point it makes contact with the outer shell. When contact is made, an external pressure develops on the liner outside surface.

#### A-4 OPEN-END VESSEL WITH AN INTERNAL AND EXTERNAL PRESSURE

For the case of an open-end cylinder with both an internal and external pressure, the previous Lamé equations become

$$\sigma_\ell = 0 \quad (A-48)$$

$$\sigma_r = \frac{p_o - p_i}{K^2 - 1} \frac{b^2}{r^2} + \frac{p_i - p_o}{K^2 - 1} K^2 \quad (A-49)$$

$$\sigma_t = \frac{-(p_o - p_i)}{K^2 - 1} \frac{b^2}{r^2} + \frac{p_i - p_o}{K^2 - 1} K^2 \quad (A-50)$$

where  $p_o$  = external pressure, psi.

Substitution of Eqs. (A-48) through (A-50) into Eq. (A-5) for  $r = a$  yields

$$\begin{aligned} p_o^2 - \frac{(1 + 3K^2)}{2K^2} p_o p_i + \frac{p_i^2 (3K^4 + 1)}{4K^4} \\ - \frac{2\sigma_y^2 (K^2 - 1)^2}{8K^4} = 0 \end{aligned} \quad (A-51)$$

This equation expresses the relationship between the internal and external pressure for incipient yielding at the bore. Solution of Eq. (A-51) for  $p_i$  yields

$$p_i = \frac{B + \sqrt{B^2 - 4R}}{2} = p_y \quad (A-52)$$

where

$$\beta = 2P_o K^2 \left( \frac{1 + 3K^2}{1 + 3K^4} \right) \quad (A-53)$$

$$\eta = \frac{4K^2 P_o^2}{1 + 3K^4} - \frac{\sigma_y^2 (K^2 - 1)^2}{1 + 3K^4} \quad (A-54)$$

Comparison of Eq. (A-44) to Eq. (A-52) will show that a greater internal pressure is required to yield an open-end pressure vessel in the presence of an external pressure.

Equation (A-46) also applies in the plastic zone for the open-end vessel with both internal and external pressure. The only change is that the constant  $c_3$  has to be determined from the boundary condition  $\sigma_r = -P_o$  at  $r = b$ . Evaluation of the constant,  $c_3$ , as indicated and substitution of  $\sigma_r = -P_i$  at  $r = a$  into Eq. (A-46) yields

$$-\ln K = \frac{\sqrt{3}}{2} \sin^{-1} \left( -\frac{\sqrt{3}}{2} \frac{P_i}{\sigma_y} \right) - \frac{1}{2} \ln \left( \sqrt{1 - \frac{3P_i^2}{4\sigma_y^2}} + \frac{P_i}{2\sigma_y} \right) + \psi + \phi \quad (A-55)$$

where

$$\psi = -\frac{\sqrt{3}}{2} \sin^{-1} \left( -\frac{\sqrt{3}}{2} \frac{P_o}{\sigma_y} \right) \quad (A-56)$$

$$\phi = \frac{1}{2} \ln \left[ \sqrt{1 - \frac{3P_o^2}{4\sigma_y^2}} + \frac{P_o}{2\sigma_y} \right] \quad (A-57)$$

Equation (A-55) expresses the relationship between  $P_o$  and  $P_i$  for an open-end cylinder in the fully plastic state. In the presence of an external pressure, a greater internal pressure is required to maintain the cylinder in plastic equilibrium.

## A-5 TEST RIG DISCREPANCIES

In the actual setup for relining launch tubes, the liner is subjected to an internal pressure and an axial end load. The test rig setup eliminates the axial load (neglecting friction) and subjects the liner to only an internal pressure. A comparison of Eqs. (A-17) to (A-44) and (A-36) to (A-47) will show that a seven- to ten-percent greater pressure is required to reach yield conditions without the end load on the liner for  $K = b/a = 3.0/2.5 = 1.2$  and  $\sigma_y = 75,000$  psi. Consequently, the results achieved with the test rig will be conservative when applied to the actual launch tubes. That is, the pressures required to seat the liner, as determined from the test rig setup, should be slightly higher than required for the actual launch tubes.

**APPENDIX B**  
**CALCULATION OF CONTACT PRESSURE FROM**  
**MEASURED STRAIN-GAGE DATA**

Since this experiment actually measures the strain on the outside of the shell, some means of relating this to an internal (contact) pressure between the liner and shell is required. Hooke's Law for  $\sigma_\ell = 0$  and  $\sigma_r = 0$  is

$$\epsilon_t = \frac{\sigma_t}{E} \quad (B-1)$$

where

$$\epsilon_t = \text{circumferential strain}$$

Using the standard Lamé equation for a thick-wall pressure vessel with an internal pressure, Eq. (A-3), the circumferential stress at the outer surface of the shell,  $r = b$ , is

$$\sigma_t = \frac{2 P_i}{K^2 - 1} \quad (B-2)$$

Substitution of Eq. (B-2) into Eq. (B-1) yields

$$P_i = \frac{E \epsilon_t (K^2 - 1)}{2} = P_c \quad (B-3)$$

This formula will calculate the contact pressure between the liner and outer shell corresponding to the measured strain  $\epsilon_t$ .

## NOMENCLATURE

a	Inside radius of cylinder, in.
b,d	Outside radius of cylinder, in.
$c_1, c_2$	Constants of integration
$c_3$	$\ln b$ , Eq. (A-46)
E	Modulus of elasticity, psi
F	Frictional force, lb
I	Moment of inertia, in. <sup>4</sup>
ID	Inside diameter
in.	Inches
K	Ratio of outside radius to inside radius
kips	Kilopounds
ksi	Kilopounds per square inch
$\ell$	Length of liner, in.
lb	Pounds
N	Force perpendicular to the sliding surface, lb
OD	Outside diameter
$p_b$	Burst pressure, psi
$p_c$	Experimentally determined contact pressure, psi
$p_f$	Full-wall yield pressure, psi
$p_i$	Internal pressure, psi
$p_o$	Theoretical external pressure, psi
$p_y$	Pressure just sufficient to cause bore yielding, psi
$p_{cd}$	Contact pressure calculated from a known radial interference, psi
$p_{ce}$	Contact pressure calculated from a known residual strain, psi
$p_\rho$	Pressure to cause yielding to a radius, $\rho$ , psi
$p_{auto}$	Autofrettage pressure, psi
psi	Pounds per square inch
r	Arbitrary radius, in.
T	Time, hr

u	Radial deflection, in.
y	Required deflection, in.
B	Arbitrary function, Eq. (A-53)
Δ	Difference
δ	Radial interference, in.
ε	Strain ( $\mu$ in./in.)
$\epsilon_R$	Residual circumferential strain ( $\mu$ in./in.)
η	Arbitrary function, Eq. (A-54)
μ	Coefficient of friction
$\mu$ in./in.	Microinches/inch
ν	Poisson's ratio
π	Constant = 3.14
ρ	Radius of plastic front, in.
σ	Stress, psi
$\sigma_u$	Material ultimate strength, psi
$\sigma_y$	Material yield strength, psi
φ	Arbitrary function, Eq. (A-57)
ψ	Arbitrary function, Eq. (A-56)

**SUBSCRIPTS**

l	Longitudinal
r	Radial
t	Circumferential